

Chapter 3

DYES, PIGMENTS AND SUPERCRITICAL FLUIDS: SELECTION OF EMERGING APPLICATIONS

M. D. Gordillo¹, C. Pereyra and E. J. Martínez de la Ossa

Department of Chemical Engineering, Food Technology and Environmental
Technologies, Faculty of Sciences, University of Cádiz,
11510 Puerto Real (Cádiz), Spain

ABSTRACT

The textile industry uses large amounts of water in its dyeing processes. Due to environmental problems the supercritical dyeing process has been developed. In this process supercritical carbon dioxide is used as the solvent for dyes.

On the other hand, pigments, used in the formulation of paints, inks, toners and photographic emulsions can be micronized by supercritical antisolvent process. Their production in form of micrometric particles with controlled particle size distribution can largely improve their characteristics.

For these reason, in the last years, supercritical fluids more and more have been proved as environmentally benign media for dyeing processes and as antisolvent to control the formation of micrometric particles.

The physico-chemical properties of supercritical fluids are halfway between those of gases and liquids; more these properties can be easily modified by a simple variation of pressure or/and temperature. Therefore, supercritical fluids can be used to develop solventless or solvent reduced processes and their mass transfer properties are useful to produce micronized particles with controlled size and distribution.

In this field, the publications appeared over the past years could be reviewed under two groupings, one involving the measurements of solubilities of dyes in supercritical carbon dioxide, with and without co-solvent, and supercritical CO₂ dyeing of fibre, and the other involving the micronization of dyes with narrow particle size distribution using a supercritical antisolvent process. In the following, a lot of recent papers will be cited, which should give an overview of actual results on solubility and precipitation of dyes in supercritical carbon dioxide.

¹ Phone: 956016458. Fax: 956016411. E-mail: dolores.gordillo@uca.es.

1. INTRODUCTION

A supercritical fluid can be defined as a substance above its critical temperature and pressure. Under this condition the fluid has unique properties, in that it does not condense or evaporate to form a liquid or gas. Although a number of substances are useful as supercritical fluids, carbon dioxide has been the most widely used supercritical CO₂ gives an option avoiding water discharge; it is low in cost, non-toxic and non-flammable. It has low critical parameters (31 °C, 73.8 bar) and the carbon dioxide can also be recycled (Özcan et al., 1998).

Supercritical fluids have a great potential for wide fields of processes: extraction processes with supercritical fluids, fractionation of products, dyeing of fibres, treatment of contaminated soils, and production of powders in micron and submicron range and reactions in or with supercritical fluids (Marr and Gamse, 2000).

An emerging technology is waterless supercritical fluid textile dyeing using supercritical carbon dioxide as the solvent medium. The large quantity of water used during the dyeing process results in a large volume of wastewater that contains not only all of the auxiliary agents but also great remains of the dye. The use of the supercritical dyeing technique circumvents the needs for water and wastewater treatment in the dyeing process. In addition, the fibres that are dyed in the supercritical fluid are completely dry after reducing the pressure to atmospheric conditions, thus recluding the requirement of drying step associated (Saus et al., 1993).

Supercritical dyeing requires studies of phase equilibrium between dyes and the supercritical solvent. For this reason, we have undertaken a review of solubility of dye in supercritical fluids.

On the other hand, nanometric or submicron pigment particles are essential materials for use in photo resists, which are used for fabricating color filters and for color liquid crystal displays. Instead of traditional mechanical milling, the supercritical anti-solvent process may provide an innovative route to meet this demand ultra-fine particles formation of pigments in different phase regions via a supercritical anti-solvent process (Wu et al., 2007).

This review is the first comprehensive review specifically focused on dyes and supercritical fluids. The review is presented in subsections according to the type of article: solubility of dyes, dyeing process and precipitation of pigments.

2. SOLUBILITY

Over the last few decades, the solubilities of solids and liquids in supercritical fluids (SCF) have been measured extensively. Such information forms an important part of establishing the technical and economic feasibility of any supercritical fluid process. Most of the investigations on solubility have been concerned with binary systems consisting of a single solute in contact with a single SCF.

In the 90s until now, many articles of solubility of dyes were published. For example, Özcan et al. measured the solubilities of eight disperse dyes in supercritical CO₂ (Özcan et al., 1997), the solubility of anthraquinone and azo dyes in supercritical CO₂ was measured by Joung and Yoo. The anthraquinone dyes showed higher solubility than the azo dyes (Joung and Yoo, 1998). Investigations on the solubility of anthraquinone dyes in supercritical carbon

dioxide were carried out by Warner et al. (Warner et al., 1999). Lee et al. measured the solubility of disperse dyes, C.I. Disperse Red 60 and C.I. Disperse Orange 3 in supercritical carbon dioxide (Lee et al., 1999). Again, the solubility of C.I. Disperse Red 60 and C.I. Disperse Blue 60 in supercritical carbon dioxide was measured by Sung and Shim (Sung and Shim, 1999). Guzel and Akgerman measured solubilities of two disperse dyes (C.I. Disperse Yellow 7, C.I. Disperse Oranges 11) and three mordant dyes (C.I. Mordant Brown, C.I. Mordant Yellow 12, and C.I. Mordant Red 11) (Guzel and Akgerman, 1999). Lee et al. published the solubility in supercritical carbon dioxide of two disperse dyes, C.I. Disperse Blue 3 and C.I. Disperse Blue 79 (Lee et al., 2000). Draper et al. measured the solubility of ten disperse dyes in supercritical carbon dioxide, and obtained results were used to develop correlations between disperse dye structures and supercritical CO₂ solubility (Draper et al., 2000). Tuma et al. compared solubility of several anthraquinone disperse dyes in near- and supercritical fluids (Tuma et al., 2001). Solubilities of Blue 79, Red 153, and Yellow 119 in supercritical carbon dioxide were measured by Lin et al. (Lin et al., 2001). In 2002, Mishima et al. measured the solubilities of azo dyes and anthraquinone in supercritical carbon dioxide (Mishima et al., 2002). In 2003, Lee et al. studied cosolvent effects on the solubilities of disperse dyes of blue 79, red 153 and yellow 119 in supercritical carbon dioxide (Lee et al., 2003). The experimental results showed how the solubilities increased by adding ethanol in supercritical carbon dioxide. Shinoda and Tamura measured solubilities of C.I. Disperse Red 1, C.I. Disperse Red 13, C.I. Disperse Orange 25 and C.I. Disperse Blue 354 in Supercritical CO₂ (Shinoda and Tamura, 2003a; Shinoda and Tamura, 2003b).

In 2003, we published the solubility of Disperse Blue 14 in supercritical carbon dioxide (Gordillo et al., 2003). Experimental solubility data as mole fraction for Disperse Blue 14 in supercritical carbon dioxide at 313, 333 and 353 K and 100- 350 bar were measured. The Disperse Blue 14 solubility always increases as the pressure does. The solubility behavior with temperature is more complex. At pressures of 100 and 150 bar, the solubility behavior with temperature is not clear. For pressures above 150 bar, the solubility increases with increasing temperature. This solubility trend is consistent with those observed by different authors for different dyes, for example Joung et al. and Draper et al. (Joung et al., 1998; Draper et al., 2000). Joung et al. measured the solubility of the same dye. The data reported by the aforementioned authors are also shown in the paper.

In 2004, Ferri et al. measured the solubilities of C.I. Disperse Orange 3, Red 324, Blue 79 and quinizarin in supercritical carbon dioxide with a flow method. Experimental data for Disperse Orange 3 were also compared with similar results obtained by the authors using a batch method in a previous work. The comparison of the results showed how the flow method reveals to be the simplest and more efficient technique to evaluate dye solubility in supercritical fluids (Ferri et al., 2004). In 2004, binary and ternary solubilities of C.I. Disperse Blue 134, C.I. Disperse Yellow 16 and their dye mixture in supercritical carbon dioxide were measured by a flow-type apparatus by Tamura and Shidona again (Tamura and Shidona, 2004). Baek et al. published the solubility of C.I. Disperse Orange 30 dye in CO₂ measured by using a batch solid-fluid equilibrium apparatus (Baek et al., 2004). Fasihia et al. investigated on solubilities of some disperse azo dyes in supercritical carbon dioxide. The measurements were performed using a simple static method. As evidenced from the experimental results, the solubilities increase with increasing density of supercritical CO₂ and the higher the melting point, the lower the solubility (Fasihi et al. 2004). Lin et al. measured

solubilities of disperse dyes of Blue 79:1, Red 82 and modified Yellow 119 in supercritical carbon dioxide and nitrous oxide (Lin et al., 2004).

In 2005, Bao and Dai published relationships between the Solubility of C. I. Disperse Red 60 and uptake on poly(ethylene terephthalate) (PET) in Supercritical CO₂. In this work the solubilities of C. I. Disperse Red 60 in supercritical CO₂ at different temperatures and pressures were measured. As all paper, the results showed that the solubilities were increasing with increasing pressure or density at constant temperature. To reveal the relationships between dye solubility and its uptake on the fibre, Bao and Dai carried out dyeing of PET fibre in supercritical CO₂ at corresponding pressures and temperatures. The results showed that very high solubility was not beneficial for high dye uptake because the dyeing of PET in SC-CO₂ also obeyed the partition rule as in water (Bao and Dai, 2005).

For the design of supercritical fluid dyeing process, it is essential to have a sound knowledge of the solubilities of dyes and the accurate solubility representation. This representation can be based on thermodynamic equations or empirical equation.

In 2005, we published solubility estimations for Disperse Blue 14 in supercritical carbon dioxide. In this paper, the solubility values of Disperse Blue 14 in supercritical CO₂ published in our previous work (Gordillo et al., 2003) were correlated with fairly good accuracy using a model based on thermodynamic aspects and the use of equations of state. The results obtained in predicting the solubility show that the choice of group contribution method (GCM) has a greater influence than the choice of one of the three equations of state investigated (Gordillo et al., 2005). Huang et al. employed four semiempirical density-based models to correlate solubilities of 32 dyestuffs in supercritical carbon dioxide. The results show that these models perform very well with three temperature-independent parameters and could be applied for satisfactory solubility predictions (Huang et al., 2005).

Recently, Tabaraki et al. related the solubility of 21 azo dyes in supercritical carbon dioxide with several descriptors over a wide range of pressures and temperatures. The prediction ability of the model was also evaluated for five azo dyes, the molecules and data of which were not in any previous data sets (Tabaraki et al., 2007). Cabral et al proposed a new methodology which correlates the dye solubility in supercritical CO₂. This methodology uses the expanded liquid model, which the solid–fluid equilibrium is modeled using the Margules model. The experimental dye solubility of CI disperse red 60, CI disperse orange 3, CI disperse blue 3, and CI disperse blue 79 in supercritical carbon dioxide were used for evaluating this new methodology. The results obtained using the proposed technique showed good agreement with the experimental data used (Cabral et al., 2007). Numerous articles of estimation of properties and correlation of solubility data of dyes can be found in the bibliography. In this work only the articles of solubility are mentioned not to extend the content of the same one.

With respect to the solubility, it is fully proven that the addition of a small amount of an organic solvent as ethanol can remarkably increase the solubility of a variety of solid solutes in the supercritical fluid (Banchero et al., 2006; Li et al., 2003; Ke et al., 1996; Chafer et al., 2002; Kopcak et al., 2005). The supercritical condition of high temperature and pressure is necessary for supercritical fluid dyeing, at which dye can be much more solved and impregnated into the polymer fibre swelled by supercritical fluid (Bae et al., 2004). It is experimentally known that dyeing of polyester fibre in supercritical carbon dioxide can be carried out over 100 °C and 200 bar (Bae et al., 2004). For more advanced development of the supercritical dyeing process, the dyeing process must be performed possibly at lower

pressure. Many investigators had reported that the solubility of disperse dye with high-molecular weight in supercritical carbon dioxide is remarkably increased by adding a small amount of co-solvent (Bae et al., 2004).

Bae et al. (Bae et al., 2004) estimated the solubility of solute in ternary supercritical fluid + solute + co-solvent mixture by using an expanded liquid model that is considered the supercritical fluid as a liquid phase. The effect of co-solvent concentration on the solubility of solute in a supercritical mixed solvent can be predicted by the model. They reported solubility measurements of disperse Red 60 in a mixture of CO₂ and co-solvents but the comparison between data with and without co-solvents was not carried out. Banchero et al. (Banchero et al., 2006) published the experimental investigation of the solubility of three disperse dyes in a mixture of CO₂ and ethanol as well as a comparison with the corresponding solubilities without co-solvent presented in previous works (Ferri et al., 2004; 2004a).

Recently, the solubility of various dispersed dyes (C. I. Disperse Red 60, Blue 56, and Yellow 54, C. I. Disperse Red 360, Blue 79, and Yellow 114) in supercritical carbon dioxide was measured by Kim et al. (Kim et al., 2006) and, subsequently, based on the solubility data, the dry dyeing was conducted in a temperature range of 363.15-423.15 K and at pressures of 10-30 MPa. Solubility data of the dispersed dyes in CO₂ were correlated in terms of the density of carbon dioxide, using an empirical equation of Bartle et al. The highest color depth of the dyed fibre was obtained when the experiment was performed at 423.15 K and 30 MPa.

Solubility of Acid Red 57 (AR57), which is an anionic dye, in supercritical CO₂ was investigated by Özcan and Özcan (Özcan and Özcan, 2006) using an ion-pairing with dodecyltrimethylammonium (DTMA) bromide. The measurements of AR57 and AR57-DTMA in supercritical CO₂ without/with methanol as a modifier solvent were carried out at temperatures from 45 to 100 °C and pressures from 250 to 325 bar. Although AR57 is insoluble in supercritical CO₂ even with methanol as a modifier solvent, AR57-DTMA can dissolve in methanol modified supercritical CO₂. The hydrophobic ion-pairing provides a possibility for the solubility of hydrophilic dye in supercritical CO₂.

3. DYEING PROCESS

In recent, waterless dyeing that used the supercritical carbon dioxide as an alternate solvent instead of water in conventional dyeing process had been gaining much interest in the textile industry for environmental reasons. Conventional dyeing process of PET fibre discharges much waste water that is contaminated by various kinds of dispersing agents, surfactants and unused dye. It is very difficult that a conventional biological process treats the wastewater including many additives. The dyeing technique with supercritical fluid is an alternative one which has been developed without environmental contamination since early 1990s. Schollmeyer and coworkers did the pioneering works for the process (Park and Bae, 2002). Saus et al. (Saus et al., 1993) reported on dyeing of PET and polypropylene with different dyes.

In 90s, Saus et al. have published numerous papers about supercritical dyeing process: *Dyeing with supercritical carbon dioxide - an alternative to high-temperature dyeing of polyester* (1993), *Dyeing with supercritical carbon dioxide - physico-chemical fundamentals* (1993), *Dyeing with supercritical carbon dioxide* (1993), *Dyeing of textiles in*

supercritical carbon dioxide (1993), *Application of supercritical carbon dioxide in finishing processes* (1993), *Dyeing from supercritical CO₂ - fastnesses of dyeing* (1994), *Dyeing natural fibres with disperse dyes in supercritical carbon dioxide* (1994), *Determination of the dye uptake of cotton with trichromatic dyes. I. Basis of quantitative multicomponent analysis* (1994), *Dyeing with carboxyl-group-containing dyes in supercritical CO₂* (1995), *Water-free dyeing of textile accessories using supercritical carbon dioxide* (1997). (Saus et al., 1993; 1993a; 1993b; 1993c ; 1994) (Knittel et al., 1993; 1994 ;1995 ;1997) (Gebert et al., 1994).

When dyeing polyester fibres from an aqueous medium, reduction clearing of the dyed fibres is carried out to maximise wet fastness properties, thus producing further effluent problems. Reduction clearing is not necessary following disperse dyeing of polyester from supercritical carbon dioxide. Supercritical CO₂ has other advantages. The application of the dye to the fabric can be controlled and a better quality of application achieved. Densities and viscosities in supercritical fluids are less and diffusion more rapid than liquids, thus shortening the process time. The solubility of the dyes can be controlled by changing the pressure and temperature (Özcan et al., 1998).

Supercritical fluids have very low surface tension, which enables easy penetration into the fibrous structure of the textile fibres. In addition, the dissolved dyestuff can easily be separated from the supercritical fluid by simple expansion enabling recycle of the valuable dyestuff and almost completely eliminating the problems related to the wastewater contamination (Guzel and Akgerman, 2000). For these reasons, supercritical CO₂ is attractive as a solvent and transport medium for disperse dyes.

Banchero et al. from Dipartimento di Scienze dei Materiali e Ingegneria Chimica – Politecnico di Torino, Italy (Banchero et al., 2006), authors of several published papers about dye and supercritical fluids, say that since Saus et al. (Saus et al., 1993) described the process for the first time in 1992, many literature works have shown that dyeing of PET fibres using supercritical carbon dioxide could be successfully performed (Özcan and Özcan, 2005; Son et al., 2004; Park and Bae, 2002; De Giorgi et al., 2000; Bach et al., 2002). Nowadays, it is known that the dye uptake as well as the fastness are comparable with those of the traditional watery dyeing (Park and Bae, 2002) and that PET is not subjected to appreciable morphological changes during dyeing (Smole and Zipper, 2002 ; Hou et al., 2004). Studies have also been done on scale-up and a number of pilot plants have been built-up all over the world (Bach et al., 1998). In spite of this, this process seems not to be attractive to the textile industry. The reasons of this lack of interest are, of course, economic: the process is carried out at relatively high pressure, which implies high investment costs for the machinery and the training of skilled staff.

Banchero et al. affirmed that a possibility to reduce the process working pressure consists in adding little quantities of low molecular weight co-solvents to the dyeing medium. The co-solvent has a twofold effect: the enhancement of the dye solubility in the fluid (Bae et al., 2004) and the promotion of the dye uptake into the fibre (West et al., 1998).

The experience achieved by the research group of Banchero, Ferri, Manna, and Sicardi is reported in a paper entitled *Supercritical Dyeing of Textiles – From the Laboratory Apparatus to the Pilot Plant* and published in *Textile Research Journal* (Banchero et al., 2008). This work shows the results obtained for polyester textiles. Laboratory scale experiments were performed to determine the equilibrium partition of each dye between the two phases. In a second part, the pilot plant was set up. The dyeing results were successful: good

reproducibility, together with a good dye uniformity and fastness (comparable with that of the traditional process) were obtained. The maximum productivity of the pilot plant is about 5 kg/h and the total duration of the dyeing process (approximately 1.5 h) is much shorter than that of the traditional method (3–4 h). Now, synthetic and natural fibres are dyed in supercritical carbon dioxide.

Since 1992, several published paper about supercritical dyeing can be cited. Since 2000, regard to the review articles and general papers, in 2001, Golob y Tusek published *The dyeing of textiles in supercritical CO₂* (Golob y Tusek, 2001), *A pragmatic approach to supercritical fluid dyeing of textile fibres with natural dyes* was published by Mukhopadhyay and Bhattacharyya, where they reviews different techniques of supercritical fluid dyeing, solubility behaviour and performance of dyeing and natural and synthetic fibres with disperse natural textile dyes from a supercritical CO₂ medium (Mukhopadhyay and Bhattacharyya, 2001) and Hendrix published *Progress in supercritical CO₂ dyeing* (Hendrix, 2001). In 2002, Bach et al. published a paper entitled *Past, present and future of supercritical fluid dyeing technology - an overview* (Bach et al., 2002). In 2004, *Progress in Supercritical Fluid Dyeing (SFD)* and *Supercritical fluid dyeing (SFD): A green technology* were published by Sayem and Rossbach (Sayem and Rossbach, 2004a y 2004b). In 2005, Malik and Kaur published a paper entitled *Supercritical carbon dioxide-The dyeing technique of future* (Malik and Kaur, 2005). In 2006, Zheng et al. published *Technique of dyeing in supercritical CO₂* (Zheng et al., 2006) and recently an article entitled *Supercritical fluid dyeing technology and application* has been published by Qun (Qun, 2007).

Regard to the type of fibre, initial applications of supercritical fluids in textile dyeing have been on dyeing of hydrophobic fibres with disperse dyes dissolved in supercritical carbon dioxide. Saus et al. (Saus et al., 1993) studied the dyeing of synthetic fibres such as polyesters, polyamides, polystyrene, polyacrylics with disperse dyes dissolved in supercritical CO₂. Gebert et al. (Gebert et al., 1994) investigated of dyeing of natural fibres (wool and cotton) with disperse dyes employing supercritical CO₂ as the solvent; after a special pretreatment with a modifying agent. Özcan et al. (Özcan et al., 1998) applied supercritical dyeing to natural fibres and successful dyeing of cotton were carried out. Guzel and Akgerman (Guzel and Akgerman, 2000) dyed wool fibres with mordant dyes (C.I. Mordant Brown, C.I. Mordant Yellow 12 and C.I. Mordant Red 11) dissolved in supercritical carbon dioxide.

Since 2000, in the bibliography, dyeing of synthetic and natural fibres can be found. Polylactide fibres (Wen and Dai, 2007; Bach et al., 2006), cotton (Fernández et al., 2007; Vankar et al., 2002, Vankar et al., 2001), wool (Zhang et al., 2007, Jun et al., 2005; Cegarra, 2002), acrylic fibres (Jun et al., 2005), nylon (Liao, 2005; Cegarra, 2002; Liao et al., 2000), polyester/cotton blends (Maeda et al., 2004), silk (Sawada et al., 2002), cellulose (Maeda et al., 2002), ramie (which is composed mainly of cellulose and is an age-old graceful textile material from China) (Liu et al., 2008; Liu et al., 2006), polypropylene (Tataba et al., 2001, Liao et al., 2001; Liao, 2000) and polyester fibres (polyethylene terephthalate) (Van der Kraan et al., 2007; Joshi et al., 2006; Li et al., 2006; Santos et al., 2005; Liao, 2005; Hou and Dai, 2005; Hou et al., 2004; Cegarra, 2002; Park and Bae, 2002; Tataba et al., 2001; Kawahara et al., 2001; Wang and Lin, 2001, Tusek et al., 2000; De Giorgi et al., 2000; Giessmann et al., 2000) among others.

4. PRECIPITATION

Nano-metric or submicron pigment particles are essential materials for use in photo resists, which are used for fabricating color filters and for color liquid crystal displays (Wu et al., 2007). The smaller sizes of pigment particles in the dispersion media yield superior color strength, contrast, and transmittance (Wu et al., 2005). Therefore, searching for feasible methods and favourable process parameters to produce nano-metric pigment particles with narrow particle size distribution (PSD) is technically important for the industrial applications. Instead of traditional mechanical milling, the supercritical anti-solvent (SAS) process may provide an innovative route to meet this demand (Wu et al., 2005; Reverchon et al., 1999; Jung and Perrut, 2001).

The supercritical antisolvent process uses both the high power of supercritical fluids to dissolve the organic solvents and the low solubility of the compounds in supercritical fluids (Shekunov and York, 2000) to cause the precipitation of such compounds once they are dissolved in the organic phase. The dissolution of the supercritical fluid into the organic solvent is accompanied by a large volume expansion and, consequently, a reduction of the liquid density, and therefore, of its solvent power, causing a sharp rise in the supersaturation within the liquid mixture. Because of the high and uniform degree of supersaturation, small particles with a narrow particle size distribution are expected (Dukhin et al., 2005).

Wu et al. in their paper entitle *Ultra-fine particles formation of C.I. Pigment Green 36 in different phase regions via a supercritical anti-solvent process* (2007) do a review of previous studies on pigment particle formation using supercritical techniques. They affirmed that these works are rather limited. Gao et al. (Gao et al., 1998) prepared micrometric particles of Pigment Red Lake C, C.I. Pigment Yellow 1, and C.I. Pigment Blue 15 using an SAS method. Micro-metric pigment particles of Bronze Red were produced by Hong et al. (Hong et al., 2000) with a continuous SAS apparatus. Wu et al. (Wu et al., 2005; Wu et al., 2006) extensively investigated the effects of the SAS process parameters on the PSD of C.I. Pigment Red 177 and C.I. Pigment Blue 15:6. Nano-metric or submicron particles were obtained from these studies. The precipitation kinetic parameters of Pigment Blue 15:6 were determined with the aid of the population balance theory (Wu et al., 2006). Reverchon et al. (Reverchon et al., 2005) investigated micronization of C.I. Disperse red 60 using both SAS and supercritical-assisted atomization (SAA) methods. They found that nano-metric particles could be formed using SAS, whereas micro-metric particles were produced using SAA. Wu et al. (Wu et al., 2006) developed a supercritical-assisted dispersion apparatus to C.I. Pigment Red 177 in propylene glycol monomethyl ether acetate with blended dispersants. In addition to Wubbolts et al. (Wubbolts et al., 1999) and Wu et al. (Wu et al., 2006), Reverchon et al. (Reverchon et al., 2003) found that the phase behaviour of mixtures in precipitator, rather than the mass transfer, governed SAS precipitation. As shown from their experimental results, submicron particles were produced when the mixtures of solvent + anti-solvent + solute in the precipitator were manipulated at supercritical homogeneous states during the particle formation stage (Wu et al., 2007).

REFERENCES

- Bach, E., Cleve, E., Schollmeyer, E. Past, present and future of supercritical fluid dyeing technology - an overview, *Review of Progress in Coloration and Related Topics* 32 (2002) 88-102
- Bach, E.; Cleve, E. and Schollmeyer, E. Past, present and future of supercritical fluid dyeing technology - an overview, *Review of Progress in Coloration and Related Topics* 32 (2002) 88-102
- Bach, E.; Cleve, E.; Schollmeyer, E.; Bork, M. and Korner, P. Experience with the Uhde CO₂-dyeing plant on technical scale. I. Optimization steps of the pilot plant and first dyeing results, *Melliand International* 3 (1998) 192-194
- Bach, E.; Knittel, D. and Schollmeyer, E. Dyeing poly(lactic acid) fibres in supercritical carbon dioxide, *Coloration Technology* 122 (5) (2006) 252-258
- Bae, H.W.; Jeon, J.H. and Lee, H. Influence of co-solvent on dye solubility in supercritical carbon dioxide, *Fluid Phase Equilibria* 222-223 (2004) 119-125
- Baek, J.-K.; Kim, S.; Lee, G.-S. and Shim, J.-J. Density Correlation of Solubility of C. I. Disperse Orange 30 Dye in Supercritical Carbon Dioxide, *Korean Journal of Chemical Engineering* 21 (1) (2004) 230-235
- Banchero, M., Sicardi, S.; Ferri, A.; Mann, L., Supercritical dyeing of textiles-From the laboratory apparatus to the pilot plant, *Textile Research Journal* 78(3), 2008, 217-223
- Banchero, M.; Ferri, A.; Manna, L. and Sicardi, S. Solubility of disperse dyes in supercritical carbon dioxide and ethanol, *Fluid Phase Equilibria* 243 (1-2) (2006) 107-114
- Bao, P. and Dai, J. Relationships between the solubility of C. I. disperse red 60 and uptake on PET in supercritical CO₂, *Journal of Chemical and Engineering Data* 50 (3) (2005) 838-842
- Cabral, V. F.; Santos, W. L. F.; Muniza, E. C.; Rubira, A. F. and Cardozo-Filho, L. Correlation of dye solubility in supercritical carbon dioxide, *J. of Supercritical Fluids* 40 (2007) 163-169
- Cegarra, J. Dyeing textile fibres in supercritical carbon dioxide [Tintura de fibras textiles en dióxido de carbono supercrítico], *Revista de la Industria Textil* 398 (2002) 77-84
- Chafer, A.; Berna, A.; Monton, J.B. and Munoz, R. High-pressure solubility data of system ethanol (1) + epicatechin (2) + CO₂ (3), *Journal of Supercritical Fluids* 24 (2002) 103-109
- Chang, K.H.; Bae, H.K. and Shim, J.J. Dyeing of pet textile fibres and films in supercritical carbon dioxide, *Korean J. Chem. Eng.* 13 (1996) 310-316
- De Giorgi, M. R.; Cadoni, E.; Maricca, D. and Piras, A. Dyeing polyester fibres with disperse dyes in supercritical CO₂, *Dyes and Pigments* 45 (2000) 75-79
- Draper, S.L.; Montero, G.A.; Smith, B. and Beck, K. Solubility relationships for disperse dyes in supercritical carbon dioxide, *Dyes and Pigments* 45 (3) (2000) 177-183
- Dukhin, S. S.; Shen, Y.; Dave, R. and Pfeffer, R. Droplet mass transfer, intradroplet nucleation and submicron particle production in two-phase flow of solvent-supercritical antisolvent emulsion, *Colloid Surf. A: Physicochem. Eng. Aspect.* 261 (2005) 163
- Fasihi, J.; Yamini, Y.; Nourmohammadian, F. and Bahramifar, N. Investigations on the solubilities of some disperse azo dyes in supercritical carbon dioxide, *Dyes and Pigments* 63 (2) (2004) 161-168

- Fernandez Cid, M. V.; Buijs, W. and Witkamp, G. J. Application of molecular modeling in the optimization of reactive cotton dyeing in supercritical carbon dioxide, *Industrial and Engineering Chemistry Research* 46 (12) (2007) 3941-3944
- Ferri, A.; Banchemo, M.; Manna, L. and Sicardi, S. A new correlation of solubilities of azoic compounds and anthraquinone derivatives in supercritical carbon dioxide, *Journal of Supercritical Fluids* 32 (2004a) 27-35
- Ferri, A.; Banchemo, M.; Manna, L. and Sicardi, S. An experimental technique for measuring high solubilities of dyes in supercritical carbon dioxide, *Journal of Supercritical Fluids* 30 (1) (2004) 41-49
- Gao Y, Mulenda TK, Shi YF, Yuan WK. Fine particles preparation of red lake C pigment by supercritical fluid, *Journal of Supercritical Fluids* 13 (1998) 369
- Gebert, B.; Saus, W.; Knittel, D.; Buschmann, H.-J. and Schollmeyer, E. Dyeing natural fibres with disperse dyes in supercritical carbon dioxide, *Textile Research Journal* 64 (7) (1994) 371-374
- Giessmann, M.; Schafer, K. and Hocker, H. Dyeing of polyester/wool from supercritical carbon dioxide with disperse and disperse reactive dyes, *DWI Reports* (123) (2000) 465-469
- Golob, V. and Tusek, L. The dyeing of textiles in supercritical CO₂ [Farbenie textilu v superkritickom CO₂], *Vlakna a Textil* 8 (4) (2001) 250-253
- Gordillo, M.D.; Pereyra, C. and Martínez de la Ossa, E.J. Measurement and correlation of solubility of Disperse Blue 14 in supercritical carbon dioxide. *J. of Supercritical Fluids* 27 (2003) 31-37
- Gordillo, M.D.; Pereyra, C. and Martínez de la Ossa, E.J. Solubility estimations for Disperse Blue 14 in supercritical carbon dioxide, *Dyes and Pigments* 67 (3) (2005) 167-173
- Guzel, B. and Akgerman, A. Mordant dyeing of wool by supercritical processing, *Journal of Supercritical Fluids*, 18 (2000) 247-252
- Guzel, B. and Akgerman, A. Solubility of disperse and mordant dyes in supercritical CO₂, *Journal of Chemical and Engineering Data* 44 (1) (1999), 83-85
- Hendrix, W.A. Progress in supercritical CO₂ dyeing, *Journal of Industrial Textiles* 31 (1) (2001) 43-56
- Hong, L.; Guo, J. Z.; Gao, Y. and Yuan, W. K. Precipitation of microparticulate organic powders by a supercritical antisolvent process, *Ind Eng Chem Res* 39 (2000) 4482
- Hou, A. and Dai, J. Kinetics of dyeing of polyester with CI Disperse Blue 79 in supercritical carbon dioxide, *Coloration Technology* 121 (1) (2005) 18-20
- Hou, A.; Xie, K. and Dai, J. Effect of supercritical carbon dioxide dyeing conditions on the chemical and morphological changes of poly(ethylene terephthalate) fibres, *Journal of Applied Polymer Science* 92 (2004) 2008-2012
- Huang, Z.; Guo, Y.-H.; Sun, G.-B.; Chiew, Y.C. and Kawi, S. Representing dyestuff solubility in supercritical carbon dioxide with several density-based correlations, *Fluid Phase Equilibria* 236 (1-2) (2005) 136-145
- Joshi, A.S.; Malik, T. and Parmar, S. Supercritical carbon dioxide dyeing of polyester, *Asian Dyer* 3 (5) (2006) 51-54
- Joung, S. N.; Shin, H. Y.; Park, Y. H. and Yoo, K. Measurement and correlation of solubility of disperse anthraquinone and azo dyes in supercritical carbon dioxide, *Korean J. Chem. Eng.* 15 (1) (1998) 78.

- Joung, S.N. and Yoo, K.-P. Solubility of disperse anthraquinone and azo dyes in supercritical carbon dioxide at 313.15 to 393.15 K and from 10 to 25 MPa, *Journal of Chemical and Engineering Data* 43 (1) (1998) 9-12
- Jun, J. H.; Ueda, M.; Sawada, K.; Sugimoto, M. and Urakawa, H. Supercritical carbon dioxide containing a cationic perfluoropolyether surfactant for dyeing wool, *Coloration Technology* 121 (6) (2005) 315-319
- Jung, J. and Perrut, M. Particle design using supercritical fluids: literature and patent survey, *Journal of Supercritical Fluids* 20 (2001) 179
- Kawahara, Y.; Kikutani, T.; Sugiura, K. and Ogawa, S. Dyeing behaviour of poly(ethylene terephthalate) fibres in supercritical carbon dioxide, *Coloration Technology* 117 (5) (2001) 266-269
- Ke, J.; Mao, C.; Zhong, M.; Han, B. and Yan, H. Solubilities of salicylic acid in supercritical carbon dioxide with ethanol cosolvent, *Journal of Supercritical Fluids* 9 (1996) 82-87
- Kim, T.; Kim, G.; Park, J. Y.; Lim, J. S. and Yoo, K. P. Solubility Measurement and Dyeing Performance Evaluation of Aramid NOMEX Yarn by Dispersed Dyes in Supercritical Carbon Dioxide, *Ind. Eng. Chem. Res.* 45 (2006) 3425-3433
- Knittel, D., Saus, W., Hoger, S., Schollmeyer, E. Dyeing from supercritical CO₂ - fastnesses of dyeing, *Melliand Textilberichte* 75 (5) (1994) 388-394
- Knittel, D., Saus, W., Schollmeyer, E. Application of supercritical carbon dioxide in finishing processes, *Journal of the Textile Institute* 84 (4) (1993) 534-552
- Knittel, D.; Saus, W. and Schollmeyer, E. Water-free dyeing of textile accessories using supercritical carbon dioxide. *Indian Journal of Fibre and Textile Research* 22 (3) (1997) 184-189
- Knittel, D.; Schollmeyer, E. and Saus, W. Dyeing with carboxyl-group-containing dyes in supercritical CO₂, *Melliand Textilberichte* 76 (10) (1995) 854-858
- Kopcak, U. and Mohamed, R.S. Caffeine solubility in supercritical carbon dioxide/co-solvent mixtures, *Journal of Supercritical Fluids* 34 (2005) 209-214
- Lee, J.W.; Min, J.M. and Bae, H.K. Solubility measurement of disperse dyes in supercritical carbon dioxide, *Journal of Chemical and Engineering Data* 44 (4) (1999) 684-687
- Lee, J.W.; Park, M.W. and Bae, H.K. Measurement and correlation of dye solubility in supercritical carbon dioxide, *Fluid Phase Equilibria* 173 (2) (2000) 277-284
- Lee, M.-J.; Cheng, C.-H. and Lin, H.-M. Cosolvent effects on the solubilities of disperse dyes of blue 79, red 153 and yellow 119 in supercritical carbon dioxide, *Journal of the Chinese Institute of Chemical Engineers* 34 (2) (2003) 255-261
- Li, Q.; Zhang, Z.; Zhong, C.; Liu, Y. and Zhou, Q. Solubility of solid solutes in supercritical carbon dioxide with and without cosolvents, *Fluid Phase Equilibria*. 207 (2003) 183-192
- Li, Z. Y.; Meng, T. Y.; Zhang, X. D.; Liu, X. W.; Xia, Y. J.; Hu, D. P. and Jiang, T. Experimental research on dyeing poly(ethylene terephthalate) fibres with disperse blue 60 in supercritical carbon dioxide, *Gao Xiao Hua Xue Gong Cheng Xue Bao/Journal of Chemical Engineering of Chinese Universities* 20 (2) (2006) 203-207
- Liao, S. K. Dyeing of microdenier polyester fabric in supercritical carbon dioxide, *Indian Journal of Fibre and Textile Research* 30 (3) (2005) 324-330
- Liao, S. K.; Chang, P. S. and Lin, Y. C. Dyeing of polypropylene fibres with disperse dyes by supercritical carbon dioxide, *Seni Kikai Gakkai Shi/Journal of the Textile Machinery Society of Japan* 54 (1) (2001) 63

- Liao, S.K. Analysis on the dyeing of polypropylene fibres in supercritical carbon dioxide, *Journal of Polymer Research* 7 (3) (2000) 155-159
- Lin, H.-M.; Ho, C.-C. and Lee, M.-J. Solubilities of disperse dyes of blue 79:1, red 82 and modified yellow 119 in supercritical carbon dioxide and nitrous oxide, *Journal of Supercritical Fluids* 32 (1-3) (2004) 105-114
- Lin, H.-M.; Liu, C.-Y.; Cheng, C.-H.; Chen, Y.-T. and Lee, M.-J. Solubilities of disperse dyes of blue 79, red 153, and yellow 119 in supercritical carbon dioxide, *Journal of Supercritical Fluids* 21 (1) (2001) 1-9
- Liu, Z. T.; Sun, Z.; Liu, Z. W.; Lu, J. and Xiong, H. Benzylated modification and dyeing of ramie fibre in supercritical carbon dioxide, *Journal of Applied Polymer Science* 107 (3) (2008) 1872-1878
- Liu, Z. T.; Zhang, L.; Liu, Z.; Gao, Z.; Dong, W.; Xiong, H.; Peng, Y. and Tang, S. Supercritical CO₂ dyeing of ramie fibre with disperse dye, *Industrial and Engineering Chemistry Research* 45 (26) (2006) 8932-8938
- Maeda, S.; Hongyou, S.; Kunitou, K. and Mishima, K. Dyeing cellulose fibres with reactive disperse dyes in supercritical carbon dioxide, *Textile Research Journal* 72 (3) (2002) 240-244
- Maeda, S.; Kunitou, K.; Hihara, T. and Mishima, K. One-bath dyeing of polyester/cotton blends with reactive disperse dyes in supercritical carbon dioxide, *Textile Research Journal* 74 (11) (2004) 989-999
- Malik, S.K., Kaur, H. Supercritical carbon dioxide - The dyeing technique of future, *Man-Made Textiles in India* 48 (1) (2005) 27-32
- Marr, R. and Gamse, T. Use of supercritical fluids for different processes including new developments-a review. *Chemical Engineering and Processing* 39 (2000) 19-28
- Mishima, K.; Matsuyama, K.; Ishikawa, H.; Hayashi, K.-I. and Maeda, S. Measurement and correlation of solubilities of azo dyes and anthraquinone in supercritical carbon dioxide, *Fluid Phase Equilibria* 194-197 (2002) 895-904
- Özcan, A. and Özcan, A. S. Solubility of an acid dye in supercritical carbon dioxide by ion-pairing with dodecyltrimethylammonium bromide, *Fluid Phase Equilibria* 249 (2006) 1-5
- Özcan, A. S.; Özcan, A. Adsorption behavior of a disperse dye on polyester in supercritical carbon dioxide, *Journal of Supercritical Fluids* 35 (2005) 133-139
- Özcan, A.S.; Clifford, A.A.; Bartle, K.D. and Lewis, D.M. Dyeing of cotton fibres with disperse dyes in supercritical carbon dioxide, *Dyes and Pigments*, 36(2) (1998) 103-110
- Özcan, A.S.; Clifford, A.A.; Bartle, K.D. and Lewis, D.M. Solubility of disperse dyes in supercritical carbon dioxide, *Journal of Chemical and Engineering Data*, 42 (3) (1997), 590-592
- Park, M. W. and Bae, H. K. Dye distribution in supercritical dyeing with carbon dioxide, *Journal of Supercritical Fluids* 22 (2002) 65-73
- Qun, X. Supercritical fluid dyeing technology and application, *China Textile and Apparel* 25 (5) (2007) 76-78
- Reverchon, E. Supercritical antisolvent precipitation of micro- and nanoparticles, *Journal of Supercritical Fluids* 15 (1999) 1
- Reverchon, E.; Adami, R.; De Macro, I.; Laudani, C. G. and Spada, A. Pigment red 60 micronisation using supercritical fluids based techniques, *Journal of Supercritical Fluids* 35 (2005) 76

- Reverchon, E.; Caputo, G.; De Marco, I. Role of phase behavior and atomization in the supercritical antisolvent precipitation, *Ind Eng Chem Res* 42 (2003) 6406
- Santos, W. L. F.; Moura, A. P.; Povh, N. P.; Muniz, E. C. and Rubira, A.F. Anthraquinone and azo dyes in dyeing processes of PET films and PET knitted fabrics using supercritical CO₂ medium, *Macromolecular Symposia* 229 (2005) 150-159
- Saus, W., Hoger, S., Knittel, D., Schollmeyer, E. Dyeing with supercritical carbon dioxide (1993b), *Textilveredlung* 28 (3) 38-40
- Saus, W.; Knittel, D. and Schollmeyer, E. Dyeing of textiles in supercritical carbon dioxide, *Textile Research Journal* 63 (3) (1993c) 135-142
- Saus, W.; Cleve, E.; Denter, U.; Duffner, H. and Schollmeyer, E. Determination of the dye uptake of cotton with trichromatic dyes. I. Basis of quantitative multicomponent analysis, *Textilveredlung* 29 (1-2) (1994) 13-18
- Saus, W.; Knittel, D. and Schollmeyer, E. Dyeing of textiles in supercritical carbon dioxide, *Textile Res. J.* 63 (3) (1993) 135
- Saus, W.; Knittel, D. and Schollmeyer, E. Dyeing with supercritical carbon dioxide - physico-chemical fundamentals, *Textile Praxis* 47 (1993a) 1052-1054
- Sawada, K., Takagi, T., Jun, J.H., Ueda, M., Lewis, D.M. Dyeing natural fibres in supercritical carbon dioxide using a nonionic surfactant reverse micellar system, *Coloration Technology* 118 (5) (2002) 233-237
- Sayem, A.S.M., Roszbach, V. Progress in Supercritical Fluid Dyeing (SFD) Taiwan *Textile Research Journal* 14 (4) (2004) 259-267
- Sayem, A.S.M., Roszbach, V. Supercritical fluid dyeing (SFD): A green technology [La teinture par fluide supercritique (SFD): Une technologie verte] *Textile Journal* 121 (5) (2004) 22-25
- Shekunov, B. Y. and York, P. Crystallization processes in pharmaceutical technology and drug delivery design, *J. Cryst. Growth* 211 (2000) 122
- Shinoda, T. and Tamura, K. Solubilities of C.I. Disperse orange 25 and C.I. Disperse blue 354 in supercritical carbon dioxide, *Journal of Chemical and Engineering Data* 48 (4) (2003) 869-873
- Shinoda, T. and Tamura, K. Solubilities of C.I. Disperse Red 1 and C.I. Disperse Red 13 in supercritical carbon dioxide, *Fluid Phase Equilibria* 213 (1-2) (2003) 115-123
- Smole, M. and Zipper, P. The influence of different treatment media on the structure of PET fibres, *Materials Research Innovations* 6 (2002) 55-64
- Son, Y. A.; Hong, J. P. and Kim, T. K. An approach to the dyeing of polyester fibre using indigo and its extended wash fastness properties, *Dyes and Pigments* 61 (2004) 263-272
- Sung, H.-D. and Shim, J.-J. Solubility of C. I. Disperse Red 60 and C. I. Disperse Blue 60 in supercritical carbon dioxide, *Journal of Chemical and Engineering Data* 44 (5) (1999) 985-989
- Tabaraki, R.; Khayamian, T. and Ensafi, A. A. Solubility prediction of 21 azo dyes in supercritical carbon dioxide using wavelet neural network, *Dyes and Pigments* 73 (2007) 230-238
- Tamura, K. and Shinoda, T. Binary and ternary solubilities of disperse dyes and their blend in supercritical carbon dioxide, *Fluid Phase Equilibria* 219 (1) (2004) 25-32
- Tataba, I.; Miyagawa, S.; Lyu, J. H.; Cho, S. M. and Hori, T. Fluid density dependency of the partition coefficient of disperse dyes between synthetic fibre and supercritical CO₂ in supercritical dyeing, *Kobunshi Ronbunshu* 58 (10) (2001) 521-526

- Tuma, D.; Wagner, B. and Schneider, G.M. Comparative solubility investigations of anthraquinone disperse dyes in near- and supercritical fluids, *Fluid Phase Equilibria* 182 (1-2) (2001) 133-143
- Tušek, L.; Golob, V. and Knez, Ž. Effect of pressure and temperature on supercritical CO₂ dyeing of PET-dyeing with mixtures of dyes, *International Journal of Polymeric Materials* 47 (4) (2000) 657-665
- Van Der Kraan, M.; Cid, M. V. F.; Woerlee, G. F.; Veugelers, W. J. T. and Witkamp, G. J. Equilibrium study on the disperse dyeing of polyester textile in supercritical carbon dioxide, *Textile Research Journal* 77 (8) (2007) 550-558
- Vankar, P.S.; Tiwari, V. and Ghorpade, B. Supercritical fluid extraction: Of natural dye from Eucalyptus bark used for cotton dyeing in microwave and sonicator, *Canadian Textile Journal* 119 (5) (2002) 32-35
- Vankar, P.S.; Tiwari, V. and Ghorpade, B. Supercritical fluid extraction of natural dye from eucalyptus bark used for cotton dyeing in microwave and sonicator, *Asian Textile Journal* 10 (2) (2001) 68-70
- Wagner, B.; Kautz, C.B. and Schneider, G.M.. Investigations on the solubility of anthraquinone dyes in supercritical carbon dioxide by a flow method, *Fluid Phase Equilibria* 158-160 (1999) 707-712
- Wang, C. T. and Lin, W. F. Scouring and dyeing of polyester fibres in supercritical carbon dioxide, *Journal of Chemical Engineering of Japan* 34 (2) (2001) 244-248
- Wen, H., Dai, J. J. Dyeing of polylactide fibres in supercritical carbon dioxide, *Journal of Applied Polymer Science* 105 (4) (2007) 1903-1907
- West, B.L., Kazarian, S.G., Vincent, M.F., Brantley, N.H., Eckert, C.A., Supercritical fluid dyeing of PMMA films with azo-dyes, *Journal of Applied Polymer Science* 69 (5) (1998) 911-919
- Wu, H. T.; Lee, M. J. and Lin H. M. Precipitation kinetics of pigment blue 15:6 sub-micro particles with a supercritical anti-solvent process, *Journal of Supercritical Fluids* 37 (2006) 220
- Wu, H. T.; Lee, M. J.; Lin, H. M. Supercritical fluid-assisted dispersion of ultrafine pigment red 177 particles with blended dispersants, *Journal of Supercritical Fluids* 39 (2006) 127-134
- Wu, H. T.; Lin, H. M. and Lee, M. J. Ultra-fine particles formation of C.I. Pigment Green 36 in different phase regions via a supercritical anti-solvent process, *Dyes and Pigments* 75 (2) (2007) 328-334
- Wu, H. T.; Lee, M. J. and Lin, H. M. Nano-particles formation for pigment red 177 via a continuous supercritical anti-solvent process. *Journal of Supercritical Fluids* 33 (2005) 173
- Wu, H.T.; Lin, H.M. and Lee, M.J. Ultra-fine particles formation of C.I. Pigment Green 36 in different phase regions via a supercritical anti-solvent process, *Dyes and Pigments* 75 (2007), 328-334
- Wubbolts, F. E.; Bruinsma, O. S. L. and van Rosmalen, G. M. Dry-spraying of ascorbic acid or acetaminophen solutions with supercritical carbon dioxide, *J Cryst Growth* 198/199 (1999) 767
- Zhang, L.-G.; Wu, Z.-M. and Zhang, C. Research on dyeing effect of wool fibre with natural pigment in supercritical carbon dioxide, *Wool Textile Journal* (4) (2007) 5-7

Chapter 4

PHOTO-CONTROLLED MOLECULAR SWITCHES BASED ON PHOTOCHROMIC SPIROOXAZINE DYES

Sung-Hoon Kim^a and Sheng Wang^b

^aDepartment of Textile System Engineering, Kyungpook National University,
Daegu, 702-701, Korea

^bSchool of Chemistry Science and Technology,
Zhanjiang Normal University, Zhanjiang, 524048, P.R. China

ABSTRACT

Photochromism refers to a reversible phototransformation of a chemical species between two forms having different absorption spectra. Photochromic compounds reversibly change not only the absorption spectra but also their geometrical and electronic structures. The molecular structure changes induce physical property changes of the molecules, such as fluorescence, refractive index, polarizability, electrical conductivity, and magnetism. When such photochromophores are incorporated into functional molecules, such as polymers, host molecules, conductive molecules, liquid crystals, the properties can be switched by photo irradiation. Among of all kinds of photochromic compounds, the spirooxazine dyes (SPO) are well-known photochromic compounds that show their high fatigue resistance and excellent photostability, which is one of the most promising candidates for applications in molecular electronics such as optical memory, molecular switching devices. In this review, we describe the recent development of spirooxazine dye as photo-controlled molecular switches in molecular materials, especially photochromism of spirooxazine in single crystal phase, spirooxazine dye polymer materials as fluorescence molecular switches, electrical conductivity switches, and viscosity switches, liquid crystal switches, gel switches and so on. In addition, layer by layer self-assemble spirooxazine dye in supermolecular chemistry as a photoswitching unit is described. We mainly present specific examples from our own research, which highlight our research group's contribution.

Key words: photochromism; photoswitching; spirooxazine dye; fluorescence; liquid crystal; viscosity; conductivity;

INTRODUCTION

In recent years, molecular switches have attracted considerable interest because they hold great promises as molecular electronic and photonic devices. In contrast to commonplace switches that turn electric appliances on and off, molecular switches enable the storage of information on a molecular level, which have the potential to significantly influence the development of optical-electronic materials science and information technologies.[1] Usually, molecular switches act as switching units in various optoelectronic devices and functional materials are addressed by stimulating it with light, electricity, or chemical reagents to specifically switch the physical properties between two states. Alternatively, a photoswitch exhibits two stable and selectively addressable states. Especially, photoinduced alteration of chemical and physical properties of photochromic molecules is of great interest because of its potential applications for optoelectronic devices, such as ultrahigh-density optical data storage and photoregulated molecular switches [2].

Among various types of photochromic molecules, the spirooxazine dyes (SPO) are well-known photochromic compounds that show their high fatigue resistance and excellent photostability. The photochromism of spirooxazine dye is attributable to the photochemical cleavage of the spiro C-O bond (Figure 1), which results in the extension of π -conjugation in the colored photomerocyanine conformer and thus shifts the absorption to the visible region. The function is based on the structure changes of single molecules which reversibly change not only the absorption spectra but also their geometrical and electronic structures. The molecular structure changes induce physical property changes of the molecules, such as fluorescence, refractive index, polarizability, electrical conductivity, and magnetism [3-7].

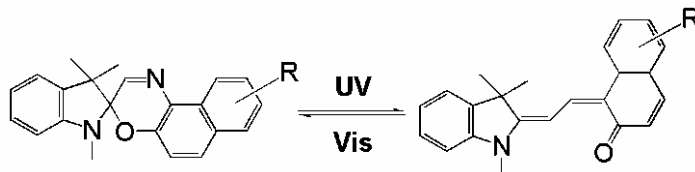


Figure 1. The photoswitching process of spirooxazine dyes

The high fatigue resistance and excellent photostability of the spirooxazine dyes in both the open-ring and closed-ring isomers makes it possible to demonstrate novel photoswitching effects, such as changes in fluorescent intensity and absorption spectra, electrochemical properties, optical rotation, magnetic properties, and electron-transfer interaction, the refractive index, dielectric constant and geometrical structure and so on[8-11]. Photoswitching of these physical properties can be accomplished by appropriate design of the molecules. By feeding back the evaluation of the physical properties to the molecular design, more sophisticated photoresponsive molecular systems can be constructed.

In generally, among the various physical properties which can be photo-switched by using spirooxazine as a photoswitching unit, molecules which change color (photochromism) and fluorescence, electrical conductivity, and viscosity upon photoirradiation, these molecular property changes can be applied to design photoswitching materials including photochromic single crystal switch, fluorescent molecular switch, conductivity switch, liquid crystal switch,

photochromic gel switch and so on. Figure 2 showed the classification of spirooxazines dye as photoswitching unit in photocontrolled molecular switches.

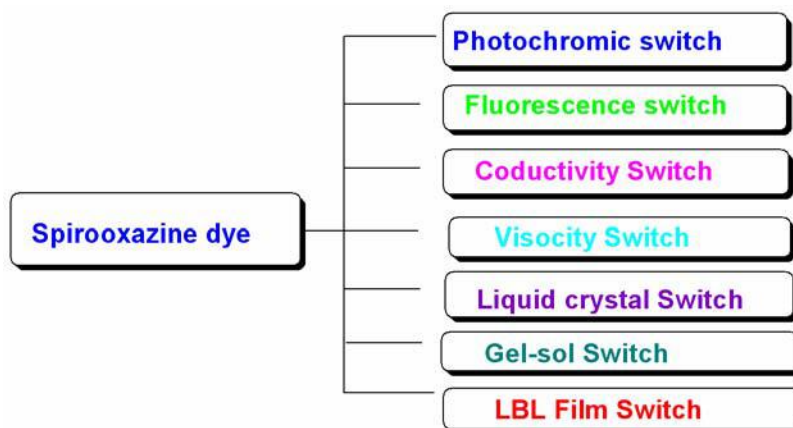


Figure 2. Classification of spirooxazine dyes as photoswitching unit

In this review, we describe recent development of spirooxazine dye as a photoswitching unit in molecular materials, especially spirooxazine single crystal photochromism, spirooxazine dye polymer materials as fluorescence molecular switch, electrical conductivity switch, and viscosity switch. In addition, layer by layer self –assemble film switch in supermolecular chemistry as a photoswitching unit. We mainly present specific examples from our own research, which highlight our research group’s contribution.

PHOTOSWITCHING OF SINGLE CRYSTAL PHOTOCHROMISM

Crystal engineering of photochromic single crystal is attractive and hot topic in recent years. The photochromism of single crystal is photochromic behavior in the solid state. The photochromic crystals switches showing thermally irreversible and fatigue-resistant characters have promising potential for optoelectronic devices such as rewritable optical memory media, optical switches, and color displays and photo-driven nano-scale actuators [12-16]. In generally, the high performance photochromic crystals switches have the following characteristic properties and functions. i) The photogenerated colored crystals exhibit dichroism under polarized light [17-18]. ii) The molecular conformations in the crystals strongly affect photocyclization and photocycloreversion quantum yields[19]. iii) Molecular structural changes following photocyclization/cycloreversion reactions induce reversible nano-scale surface morphological changes[20]. Although many photochromic compounds have been reported thus far, compounds which show photochromic reactivity in the crystalline phase are rare. Spirooxazine dyes (SPO) are known to offer remarkable stability towards photo-fatigue in solution and in various matrices, but there seldom have been reported to be photochromic spirooxazines in the crystalline state. Recently Natia L. Frank’s group synthesized a photochemically reversible, thermally irreversible isomerization of a spirooxazine dye **1** in the single crystalline phase (Figure 3) [21].

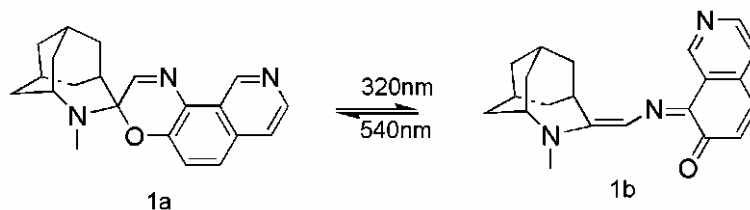


Figure 3. The photoswitching process of the spirooxazine dye **1**

The spirooxazine dye **1** was synthesized according to synthetic routes as shown in Figure 4. The effect of constrained media on the photoswitching behavior of **1** was investigated in both polymer films and the microcrystalline state. The spirooxazine dye **1** showed the excellent photochromic switching behavior in polymer films and in the microcrystalline state.

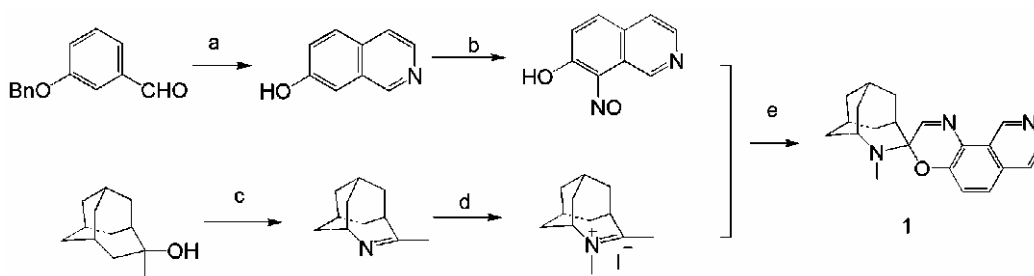


Figure 4. Synthetic routes of the spirooxazine dye **1** (a) aminoacetaldehyde dimethylacetal, trifluoroacetic anhydride, $\text{BF}_3 \cdot \text{OEt}_2$, (b) sodium nitrite, $\text{HCl}/\text{H}_2\text{O}$; (c) sodium azide, methanesulfonic acid, CH_2Cl_2 ; (d) methyl iodide, CH_2Cl_2 ; (e) Et_3N , CH_2Cl_2 .

X-ray quality single crystals of **1a** were obtained by recrystallization from hexane to give colorless monoclinic $\text{P}2_1/\text{c}$ prisms (ORTEP diagram of **1a** shown in Figure 5). The closed form (SPO) crystallizes with four molecules in the unit cell in pairs of head-to-tail dimers that sit orthogonal to each other in the crystal lattice (Figure 6).

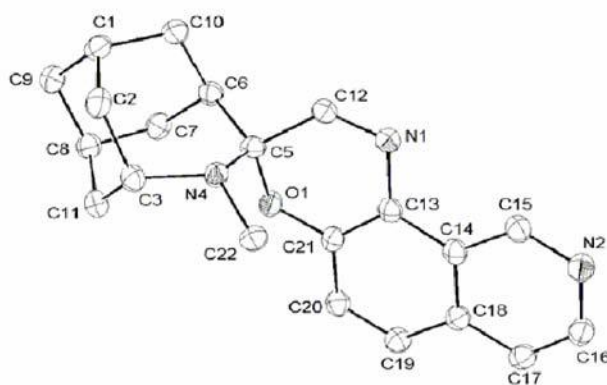


Figure 5. ORTEP diagram of **1a**. Thermal ellipsoids are shown at 50% probability. Hydrogen atoms have been omitted for clarity.

Intermolecular π - π contacts within each dimer are weak, with an intermolecular mean plane distance of 3.818 Å. Analysis of bond lengths and angles reveals little deviation from typical bond lengths and angles of other spirooxazines [22–25]. The cycle of photoisomerization is photochemically reversible, thermally irreversible, and fatigue resistant, as evidenced by numerous cycles of irradiation (>10 cycles).

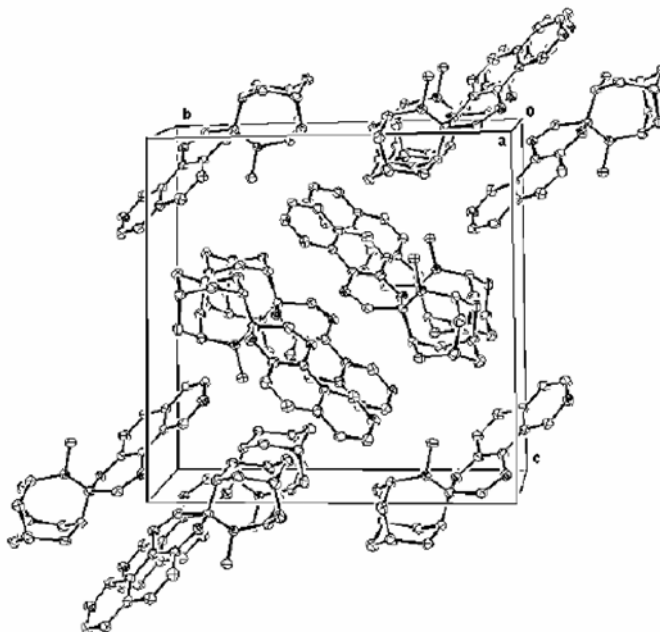


Figure 6. Packing diagram of the unit cell of the closed form of spirooxazine (**1a**). Thermal ellipsoids are shown at 50% probability. Hydrogen atoms have been omitted for clarity.

We also report herein the spirooxazine dye to exhibit photochromism both in solution and in the pure crystalline state [26]. The spirooxazine dye **2** was prepared according to the following synthetic routes (shown in Figure 7). The spirooxazine dye **2** showed the excellent photochromic switching behavior in solution and in the crystalline state.

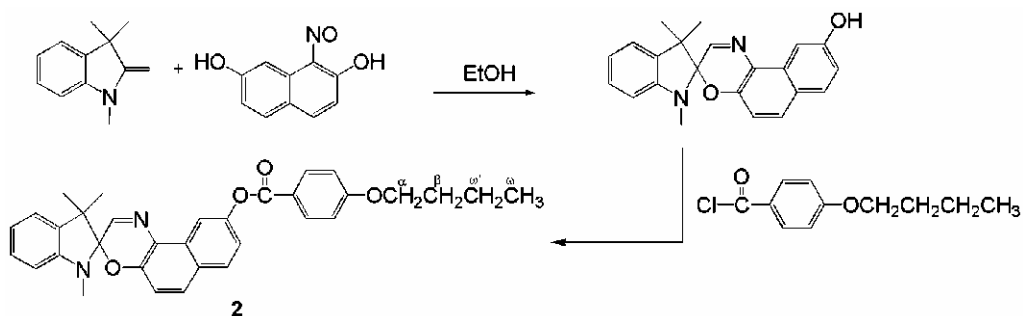


Figure 7. Synthetic routes of the spirooxazine **2**

Analysis of single crystal structure of spirooxazine dye **2**, it is evident that the molecules of the spirooxazine arrange themselves in a monoclinic crystallographic system ($C2$), unit cell

of dimensions: $a=25.421$, $b=8.298$, $c=30.567$ Å with $\beta=111.51(3)^\circ$. This closed form transforms to the coloured open form upon UV irradiation. From the ORTEP diagram, it was concluded that the spiro centre was tetrahedral (Figure 8). The crystal packing scheme is shown in Figure 9. Only the phenyl groups overlapped with face-to-face geometry, with an interplanar separation of 3.5 Å, the molecules being held together by π - π stacking interaction. The general hydrogen bond is constituted with a donor X-H and an acceptor A, in the form X-H—A. The bond may be described in terms of d , the distance between H—A, and D , the distance between X—A. The weak C-H—O hydrogen bonds have d and D separations of around 2.0–3.0 Å and 3.0–4.0 Å, respectively [27]. From the results of the intermolecular distance N2—C33=3.9 Å, the molecules are also held together through weak intermolecular hydrogen bonding.

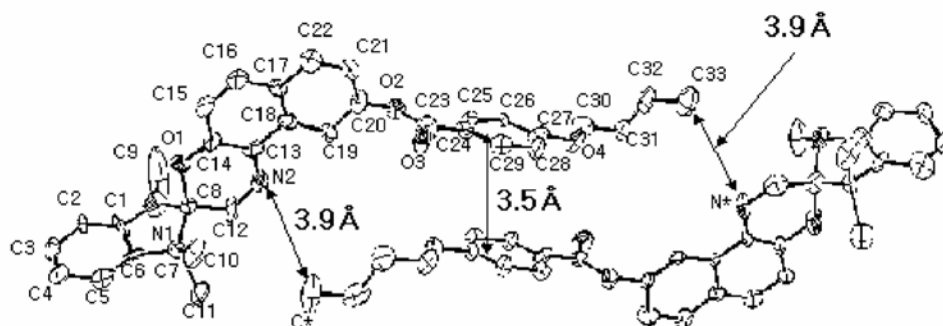


Figure 8. ORTEP view of molecular structure of spirooxazine dye 2

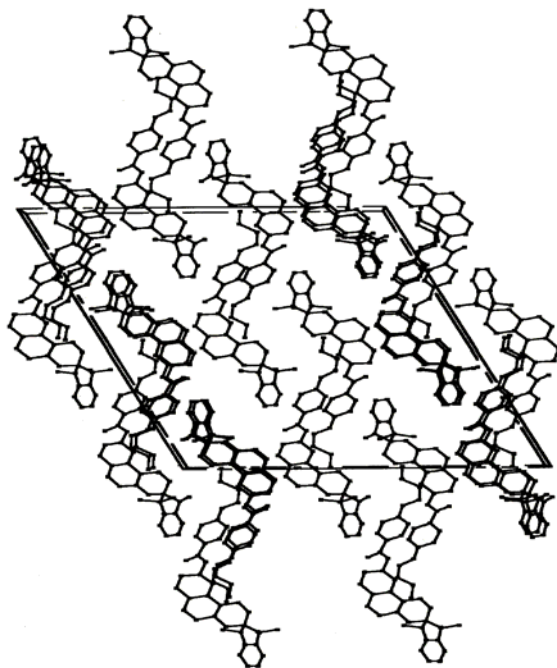


Figure 9. Crystal packing structure of spirooxazine dye 2 in unit cell

PHOTOSWITCHING OF FLUORESCENCE

Fluorescent photochromic switches attract strong interest for their possible application in optical memory as well as in fluorescent probe [28-29]. There have reported a lot of fluorescent photochromic switches including fluorescent diarylethene, spiropyran and so on. However, photocontrollable fluorescent changes of spirooxazine are very scarce [30]. Understanding the fluorescent spirooxazine photochromic reactions at a single-molecule level is very important, which can help ultimate realize the ultrahigh-density single molecule optical memory. Recently, Tian's group [31] reported a novel spironaphthoxazine molecule with a much more stable open-ring photomerocyanine form by incorporating a ferrocene moiety in the parent spirooxazine (abbreviated as SOFC) and successfully demonstrated 2D and 3D optical memory. Figure 10 represents the structure and photochemical isomerization of the novel spironaphthoxazine molecule (abbreviated as SOFC).

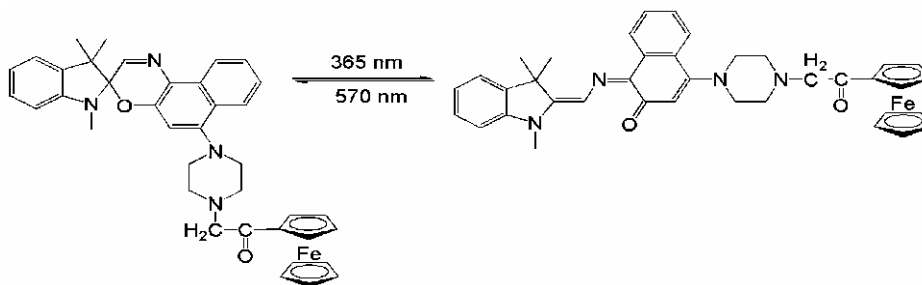


Figure 10. Photoisomerizing behavior of the spironaphthoxazine SOFC. Left: Spirooxazine Right: Photomerocyanine form

Like other spirooxazine molecules, SOFC undergoes reversible photochromic reaction. Corresponding to the difference between the UV-vis absorption before and after photoisomerization, the luminescence response of SOFC is also dictated by the binary status (Figure 11).

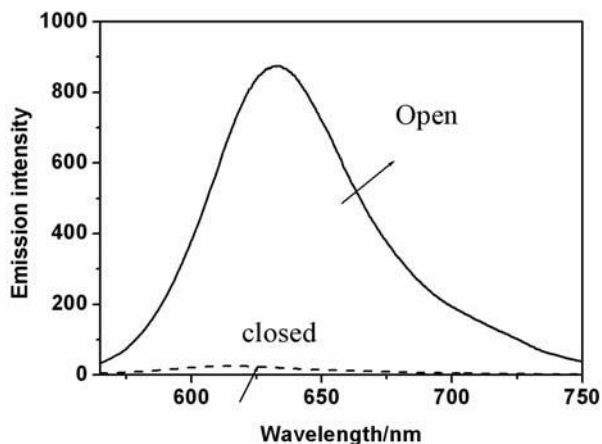


Figure 11. Emission spectra of SOFC before (broken line) and after (solid line) irradiation of the same sample

Excitation (at $\lambda=532\text{nm}$) of the closed-ring form, which has no absorption in the visible region at room temperature, produced no fluorescence emission, but the corresponding opening form luminesced strongly due to the formation of an extended π -conjugation system following the cleavage of the spiro-C-O bond. Thus, the binary data stored in the two isomers can be transduced into the fluorescence signals and read out conveniently.

In addition, The SOFC-PMMA films for imaging micrometer-sized objects in two dimensions utilizing fluorescence as the read-out method. The polymer films were prepared by spin-coating a dichloromethane solution of SOFC-PMMA mixture onto glass substrates, and then exposed to 365nm light irradiation through a mask with features in the micrometer-size regime. Subsequent to irradiation, the mask was removed and the image was successfully transferred to the polymer film as fluorescence patterns with a fine resolution. Figure 12 illustrates one such representative fluorescence image generated. The masked areas are dark and those areas exposed to 365nm light irradiation appear luminescent.

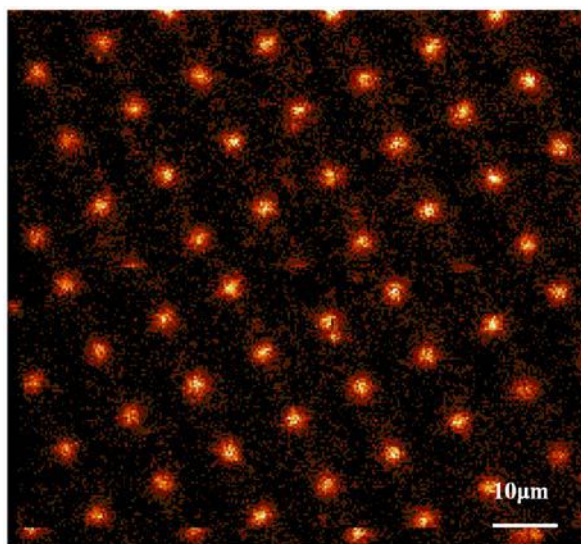


Figure 12. Fluorescence image generated from irradiation (5min) at 365nm of SOFC-PMMA film through a dot-patterned contact mask. The light regions indicate luminescence and the dark regions are non-luminescent ($\lambda_{\text{ex}}=532\text{nm}$). The size of one dot is approximately 4µm.

Dispersing the spirooxazine dye in a polymer matrix is by far the easiest strategy to prepare photochromic films. However, it has some serious limitations. Because the doped system were easily crystallization, phase separation, or the formation of concentration gradients in long-term storage. Undoped photochromic polymers would be advantageous over their dispersed monomeric counterparts because a high concentration of the active photochromic component can be incorporated into a polymer film resulting in the amplification of the desired effect, while maintaining the optical homogeneity of the material. Our group synthesized a fluorescent photochromic spirooxazine polymers switch containing carbazole (Cz) and spironaphthoxazine (SPO) moieties in the pendant groups (PMMA-Cz-SPO) (as shown in Figure 13) [32-33].

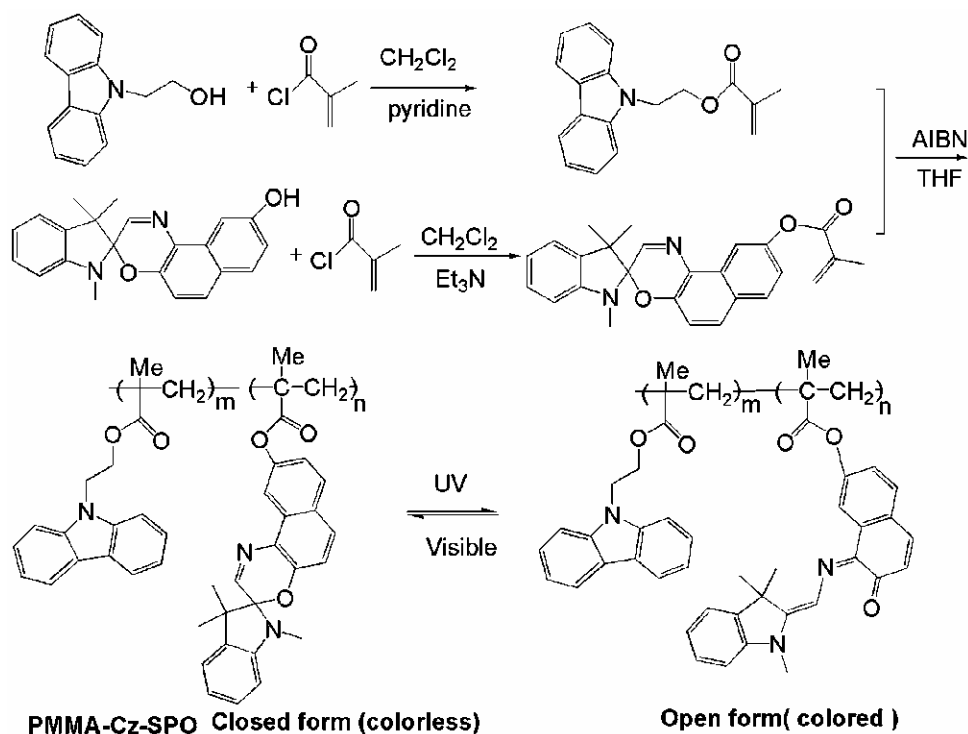


Figure 13. Synthetic routes and photoswitchable process of PMMA-Cz-SPO copolymer

The PMMA-Cz-SPO showed the excellent photochromic switching behavior in solution and in film. The PMMA-Cz-SPO copolymer exhibited photoluminescence at 348 nm and 364nm in THF solution at room temperature when excited at 320 nm. The fluorescence intensity of the copolymer decreased along with the photochromism from the ring-closed form to the ring open form irradiation with UV light (as shown in Figure 14).

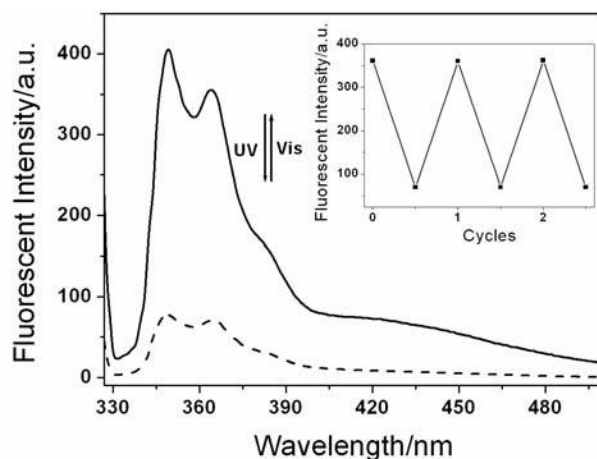


Figure 14. Fluorescence emission spectra change of PMMA-Cz-SPO copolymer in THF solution upon irradiation with UV/Vis light at room temperature. The inset figure shows the fluorescence monitoring of cycles on and off (Excited at 320nm, λ_{em} = 348nm).

The blue emission was suppressed and almost wholly quenched of the photoluminescence at the photostationary state. The original photoluminescence was also recovered within 5 seconds restored by irradiation with visible light. Figure 14 inset shows a cycling experiment in which the maximum emission of PMMA-Cz-SPO in THF solution is monitored upon alternate irradiation with UV and Visible light.

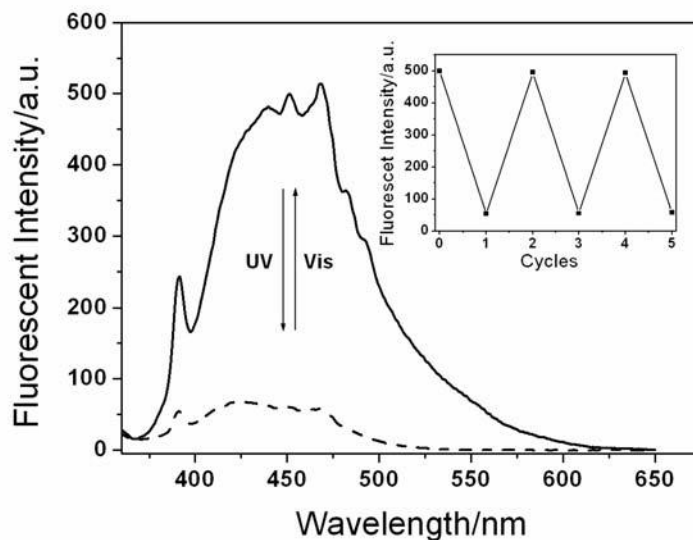


Figure 15. Fluorescence emission spectra changes of PMMA-Cz-SPO copolymer in film upon irradiation with UV/Vis light (excited at 342nm). The inset figure shows fluorescence monitoring of cycles on and off (Excited at 340nm, $\lambda_{em}=450$ nm).

Figure 15 shows the fluorescence spectra change of PMMA-Cz-SPO in film with excitation wavelength at 342 nm. The fluorescence intensity change was regulated by the photochromic reaction. Before irradiation with UV light, it showed a broad emission in the range of 400-550 nm with λ_{em} round 450 nm. Upon irradiation with UV light, the fluorescent intensity of PMMA-Cz-SPO gradually decreased and almost wholly quenched. The possible explanation for the fluorescence quenching is due to an increase in photoinduced electron transfer (PET) between the carbazole units and the spirooxazine isomers in PMMA-Cz-SPO film [34]. After irradiation with visible light, the original emission spectra are regenerated. Irradiation of photo-stationary of PMMA-Cz-SPO film with visible light led to a complete recovery of the initial fluorescence signal. From it can be seen Figure 15 inset, the fluorescence intensity reversibly changed at 450 nm (excitation: 342 nm) by alternate irradiation with UV and Visible light and this cycle could be repeated more than 10 times, which is an excellent photochromic spirooxazine fluorescence switch. The luminescence of carbazole chromophore is effectively regulated by toggling between the two isomers of the spirooxazine subunit in solid film, attributed to the change in PET between the carbazole and each form of the spirooxazine photochrome. It exhibits good photochromic properties, especially high fluorescent quantum efficiency and excellent fatigue resistance, which are promised to application all photon-mode memory media and fluorescent molecular switch.

PHOTOSWITCHING OF VISCOSITY

The photocontrolled molecules incorporated into supramolecular/macromolecular structures comprise a powerful approach towards the development of new materials and devices of nanoscale dimensions [35-36], and the control of these organisational processes by chemical or physical elements is a major challenge. A promising approach towards such responsive or smart materials is the integration of photochromic moieties into the supramolecular building blocks, which would offer the possibility to alter the self-assembly process of the individual molecules or change the properties of the supramolecular arrays by means of light [37].

A polymer having photoisomerizable unsaturated linkage in the backbone is suspected to change its conformation under photoirradiation. The change of intramolecular interactions in polymer systems induces a conformational change in the polymer chain and can be detected by viscosity measurement. Irie et al. [38] reported a viscosity change by photoirradiation of spiropyran system was observed for the first time for poly (methacrylate) with spiropyran pendant groups. A change in dipole moment due to isomerization from photochromic spiroxazine to the merocyanine form would be expected to alter intramolecular interaction of polymer chain when the spiroxazines are incorporated into the polymer pendant groups or backbone groups. We synthesized a photochromic spirooxazine copolymer which shows a photocontrolled viscosity switch (Figure 16) (abbreviated as PDDM-SPO) [39].

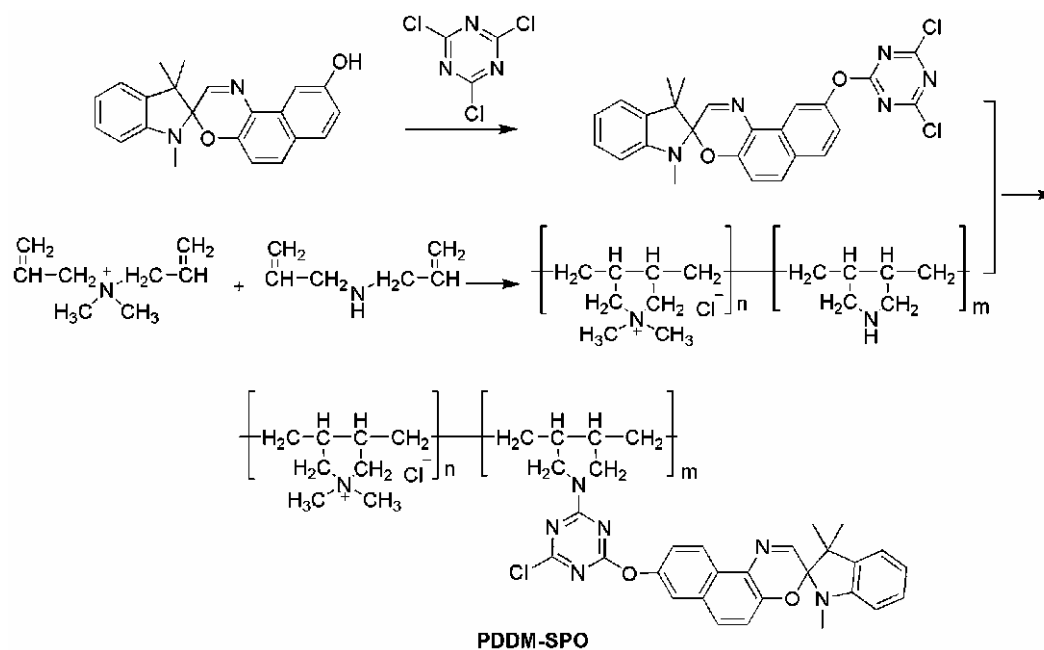


Figure 16. Synthetic routes of the PDDM-SPO polymer

We find the photochromic spirooxazine dye incorporated polymer showed excellent the photoswitching behavior of viscosity. Figure 17 shows the viscosity changes of the polymer having spiroxazine as side group in methanol before and after UV irradiation. The viscosity during UV irradiation returns to the initial value in less than 5 min at $-5\text{ }^{\circ}\text{C}$ after the light is

removed. In methanol the relative viscosity after UV irradiation is 5% lower than the viscosity in dark. The recovery cycles of the viscosity can be repeated many times without any noticeable fatigue.

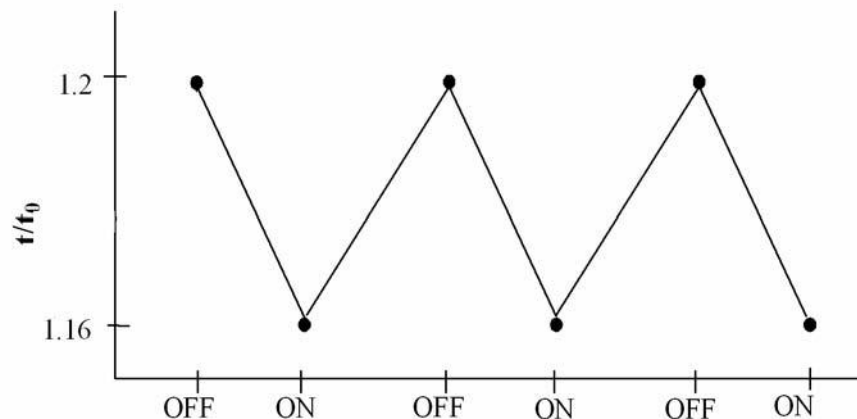


Figure 17. Change of the viscosity of a methanol solution of polymer having spirooxazine pendant group on UV irradiation at $-5\text{ }^{\circ}\text{C}$. Concentration of the polymer is 2% w/v.

These changes can be attributed to different molecular properties like shape and conformational freedom of the open and closed form of spirooxazine dye. Electrostatic attractive forces between the zwitterions and the charges on positive ammonium residues of the polymer chain tend to contract the polymer chain. In dark the attractive force considerably decreases because of the disappearance of the zwitterions structures of spirooxazine (Figure 18).

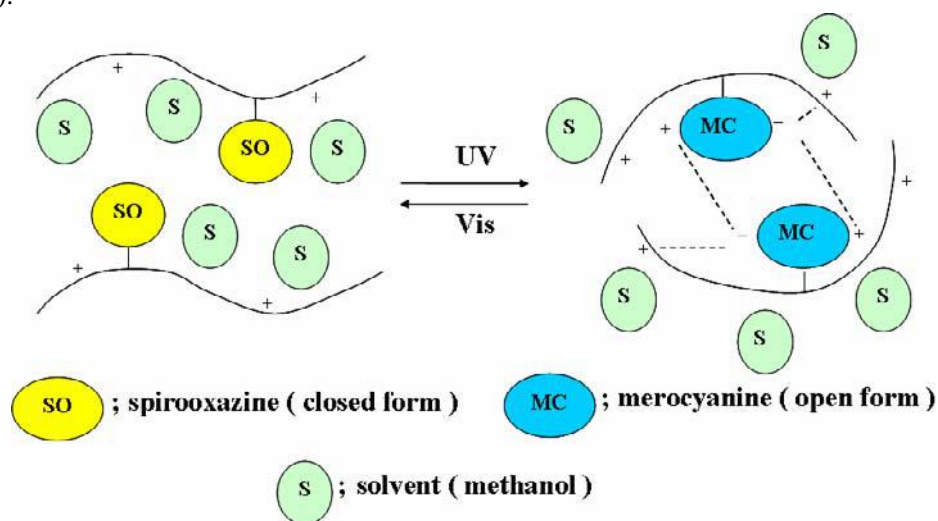


Figure 18. Schematic illustration of photostimulated conformation change of polymer chain on UV irradiation.

In addition, we calculated and simulated the photo-induced structural changes from spiro to merocyanine in order to understand the viscosity changes of the photochromic spirooxazine

polymer. Figure 19 shows the optimized photochromic spirooxazine molecular structure changes from the closed form to open form. All the theoretical calculations were performed by DMol³ program in the Materials Studio 4.2 package [40-41]. The photo-induced structural change from spiro to merocyanine causes the volume decrease, the diameter of photochromic spirooxazine polymer decreased from 32.52 Å to 29.18 Å. From the above result, we easily understand the photoswitching viscosity changes of the photochromic spirooxazine polymer. The theoretical calculations accorded with the experimental result. In addition, we investigated the other photochromic spirooxazine polymers viscosity changes, they show the excellent photoswitching viscosity behavior [33, 42].

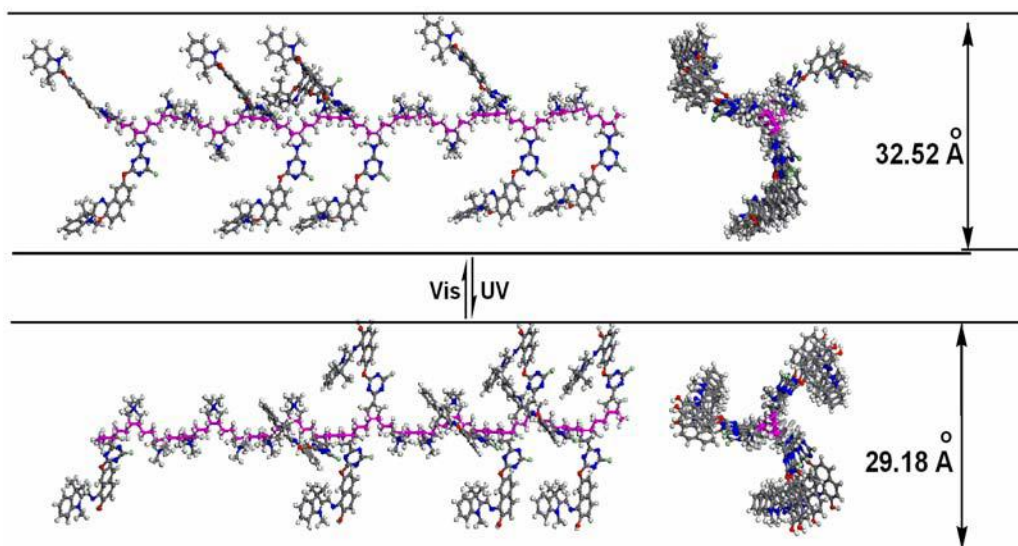


Figure 19. Calculations schematic illustration of photostimulated conformation change of polymer chain on UV/Vis light irradiation.

PHOTOSWITCHING OF CONDUCTIVITY

The design and creation of molecular systems that show chemical and physical changes in response to external stimuli is a topic of current interest because of their potential applications, as sensing and switching devices. In particular, the photo-induced electrical properties of photo-electric active materials, such as photoconductivity, have attracted considerable attention from the viewpoint of fundamental interest as well as from their practical applications. There is an important characteristic feature in the electronic structure changes of spirooxazine from the closed-form to open-form. So we hope to modulate the conductivity of spirooxazine and its derivative by light. We synthesized the a poly[N,N-[(3-dimethylamino)propyl]methacrylamide] having spirooxazine pendant group (Figure 20), which showed the excellent photochromic behavior with UV/Vis light irradiation [42].

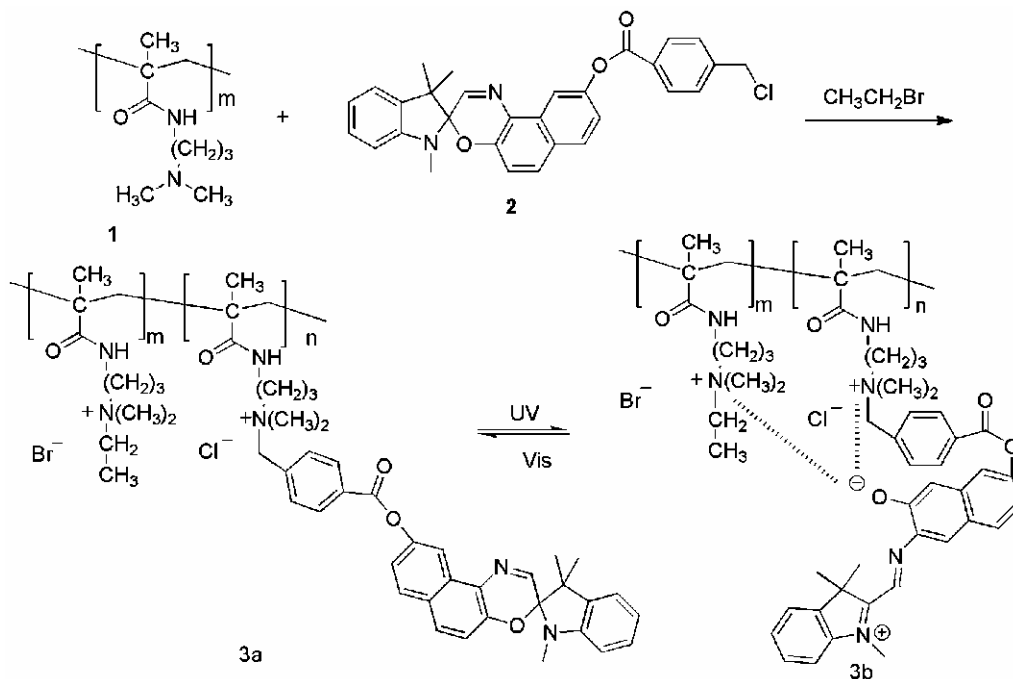


Figure 20. Synthetic routes and photoswitching process of the polymer **3**

This is a typical ionic polymer. In generally, the ionic polymers show the conductance behavior in electric field. When the spirooxazine dyes were incorporated in ionic polymer. We hope it can modulate the conductivity of the ionic polymer by light stimulation. We devised the following device to monitor the conductivity change of the ionic polymer by UV-Vis light (Figure 21).

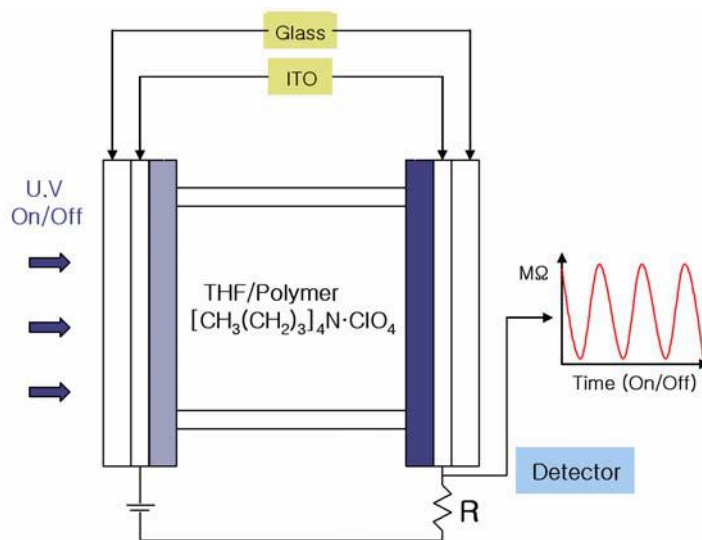


Figure 21. Schematic diagram of the conductivity measurement system

The photoinduced ionic conductivity response was analyzed at 15 °C and is shown in Figure 22. The photoinduced ionic conductivity can be estimated from the expression $(1/R_t)/(1/R_0)$ where R_0 and R_t are the resistance before and after UV irradiation. The ionic conductivity increased upon UV irradiation, which brought about the generation of zwitterions form, and subsequently decreased in dark, which in turn brought about the generation of closed spiro form. Sufficient reversibility was found in this polymer and this response was completely synchronized with that in the absorbance changes.

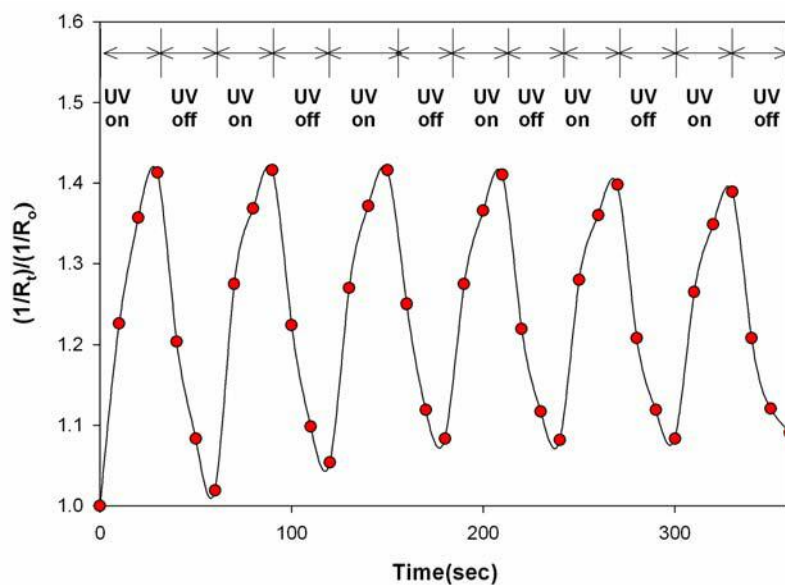


Figure 22. Photoinduced ionic conductivity response for polymer 3 at 15 °C

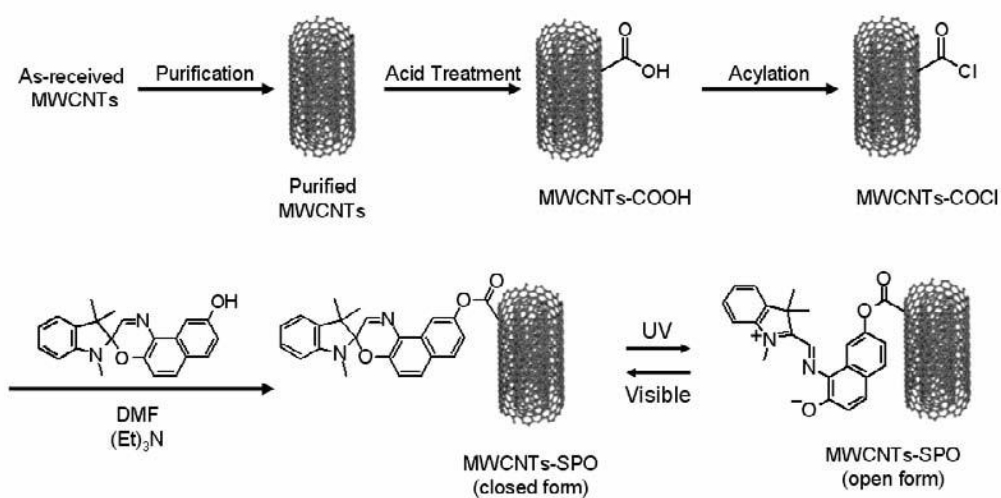


Figure 23. The synthetic routes of SPO-MWNTs.

In addition, we designed and synthesized that the photoinduced conductivity response in SPO dye molecules attached to the multi-walled carbon nanotubes (MWNTs). The preparation of covalently bonded MWNTs-SPO is depicted in Figure 23.

We demonstrate the photoinduced conductivity switch (shown in Figure 24.) The photoinduced conductivity can be also estimated from the expression $(1/R_t)/(1/R_0)$, where R_0 and R_t are the resistances before and after UV irradiation, respectively. The conductivity increased upon UV irradiation, which brought about the generation of merocyanine form. In dark the conductivity of MWNTs-SPO considerably decreased because of the disappearance of the merocyanine structure of SPO. The common feature of most intrinsically conducting organic materials is the presence of alternating single and double bonds along the entire molecule, which enables the delocalization or mobility of charge along the π -system. The conductivity is thus assigned to the delocalization of π -bonded electrons over the molecule. On UV irradiation the C-O bond of the colorless SPO is cleaved and colored merocyanine form is obtained. Thus, the interconversion between spiro form and merocyanine systems has been extensively investigated due to their potential applications in molecular devices and uses in nano- and biotechnology.

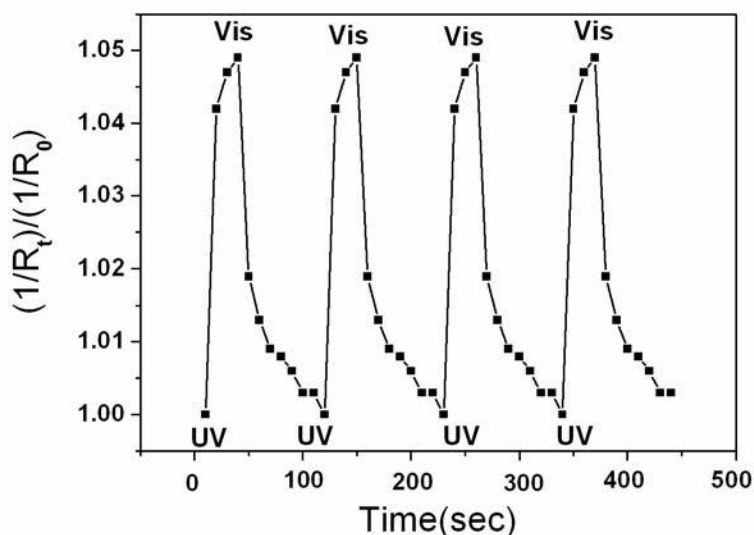


Figure 24. The photoinduced resistance changes for MWNTs-SPO thin film at 20°C.

In the merocyanine form, the electronic distribution should be described by delocalization of the π electrons with a negative charge on the oxygen and with a positive charge on the heterocyclic ring. A change in HOMO-LUMO band gap due to isomerization from spiro form to the merocyanine of SPO would be expected to alter conductivity of MWNT itself. Figure 25 shows the optimized molecular structure of the SPO and the electron distribution of its HOMO and LUMO. All the theoretical calculations were performed by DMol³ program in the MS Modeling 3.2 package which is the quantum mechanical code using density functional theory [43]. Perdew-Burke-Ernzerhof (PBE) functional of generalized gradient approximation (GGA) level [44] with double numeric polarization basis set [40] was used to calculate the

energy level of the frontier molecular orbital. The photo-induced structural change from spiro to merocyanine causes a large decrease in LUMO and a small increase in HOMO, producing a large bathochromic shift of the first band. Comparison of the electron distribution in the frontier orbitals of merocyanine reveals that HOMO-LUMO excitation moved the electron distribution from the indoline moiety to the naphthalene moiety. Excitation of the open form SPO leads to the injection of the excited electrons from the excited state dye to MWNT via naphthalene moiety connected to MWNT by an ester linkage. The recovery cycle of the conductivity before and after UV irradiation could be repeated many times without any noticeable change.

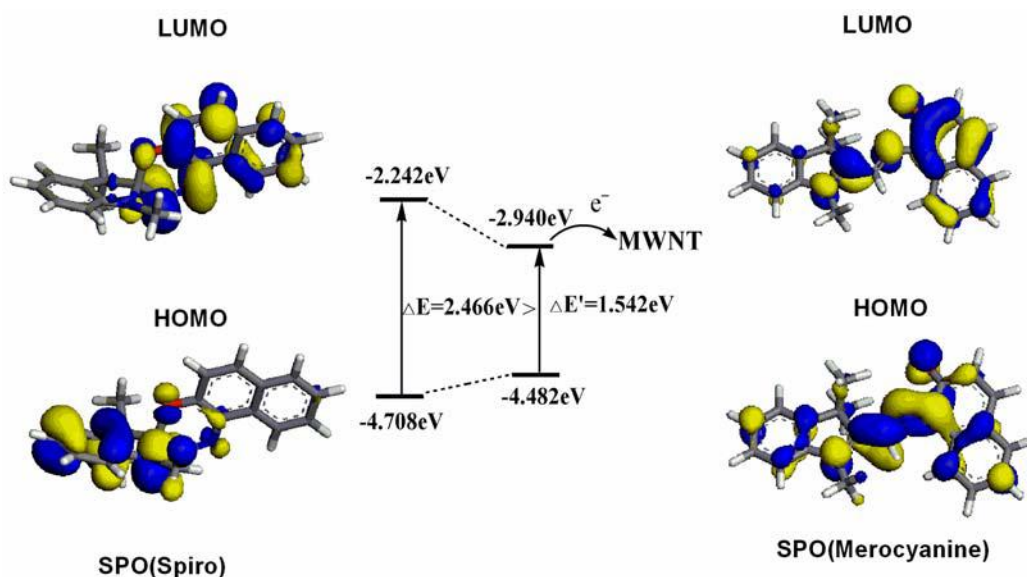


Figure 25. Electron distribution of the HOMO and LUMO energy level of SPO (Spiro) and SPO (Merocyanine).

PHOTOSWITCHING OF LIQUID CRYSTAL

The control of the structure and optical properties of liquid-crystalline (LC) phase by means of light is a major challenge in development of molecular devices and optical data storage system. So far various types of photoresponsive liquid crystals have been reported [45-46]. The combination of liquid-crystallinity and photochromic behavior in molecular systems promises to be very useful in optical technological devices. We have designed and prepared a new spirooxazines photochromic liquid crystal switch (as shown in Figure 26) [47].

We demonstrate that the photoswitching process of spirooxazines dye liquid crystal and optimize the the closed-form and closed form of spirooxazines dye liquid crystal (Figure 27). All the theoretical calculations were performed calculations were performed by DMol³ program in the MS Modeling 3.2 package. From the Figure 27 can be seen that the molecular structure of spirooxazine dye liquid crystal change a large by UV/Vis light irradiation.

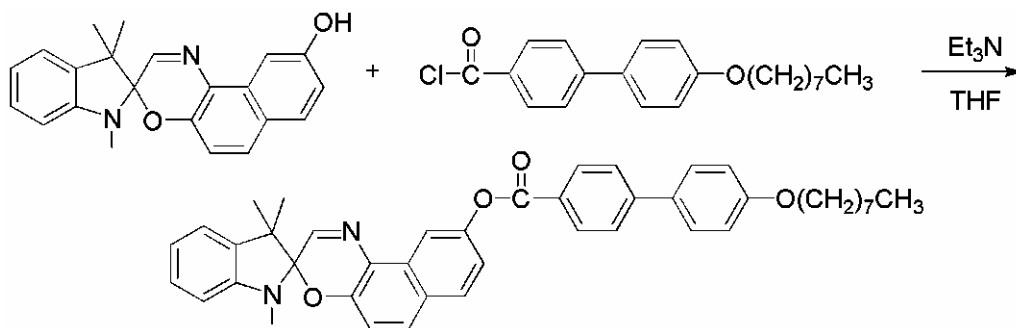


Figure 26. The synthetic route of SPO liquid crystal.

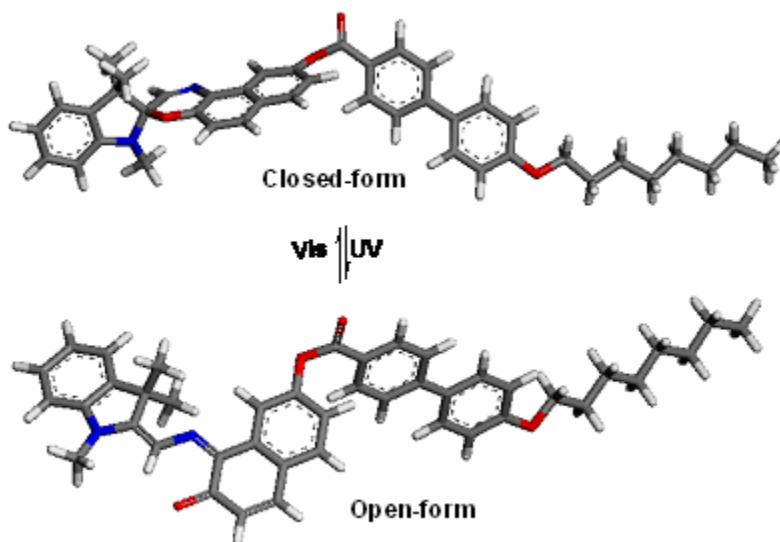


Figure 27. The photoswitching process of spirooxazine dye liquid crystal

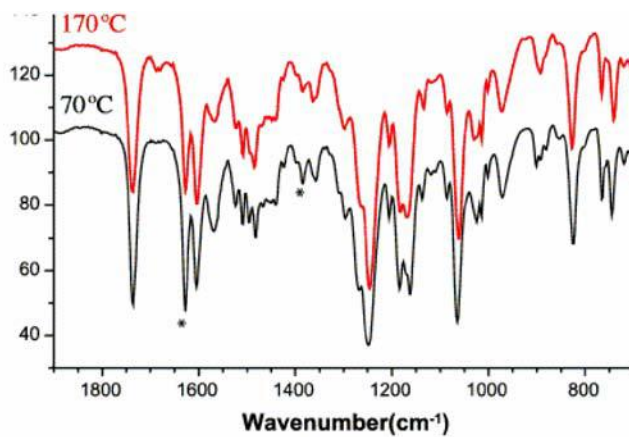


Figure 28. FT-IR spectra of the SPO liquid crystal. during heating

To conform the structural changes of the SPO liquid crystal, the FT-IR spectra of the compound were monitored by as shown in Figure 28. Due to ring opening reaction of the spiroxazine, the chromophoric structure changes to a form of merocyanine. This structural changes reflect in IR spectra; the C=N stretching band at 1628 cm^{-1} and the CH_3 deformational stretching band in O-linkage at 1384 cm^{-1} were markedly decreased at $170\text{ }^\circ\text{C}$.

DSC data also showed that SPO liquid crystal demonstrated a phase transition with a low ΔH (about 4.0 mJ/g) at $\sim 65\text{ }^\circ\text{C}$ during the cooling and heating cycle following the nematic–isotropic phase transition as indicated in Figure 29.

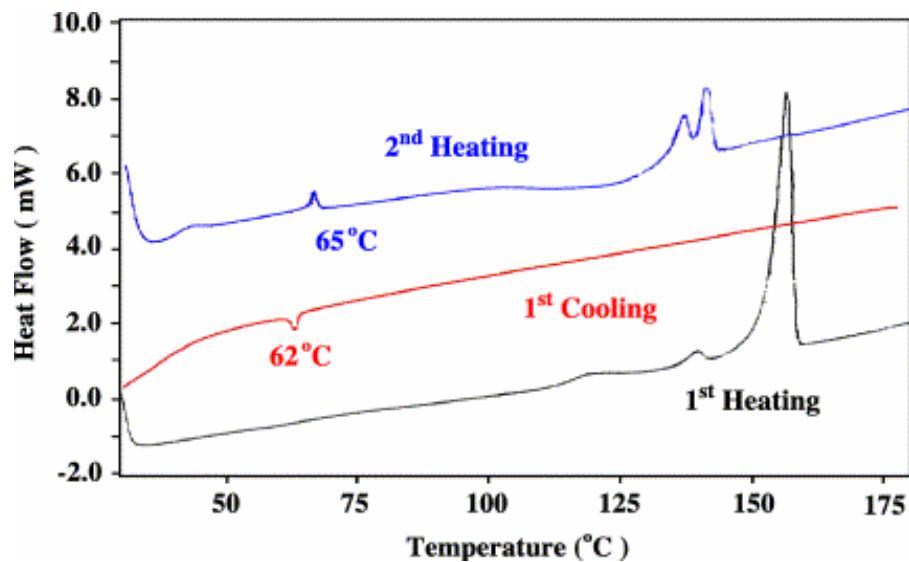


Figure 29. DSC data of SPO liquid crystal.

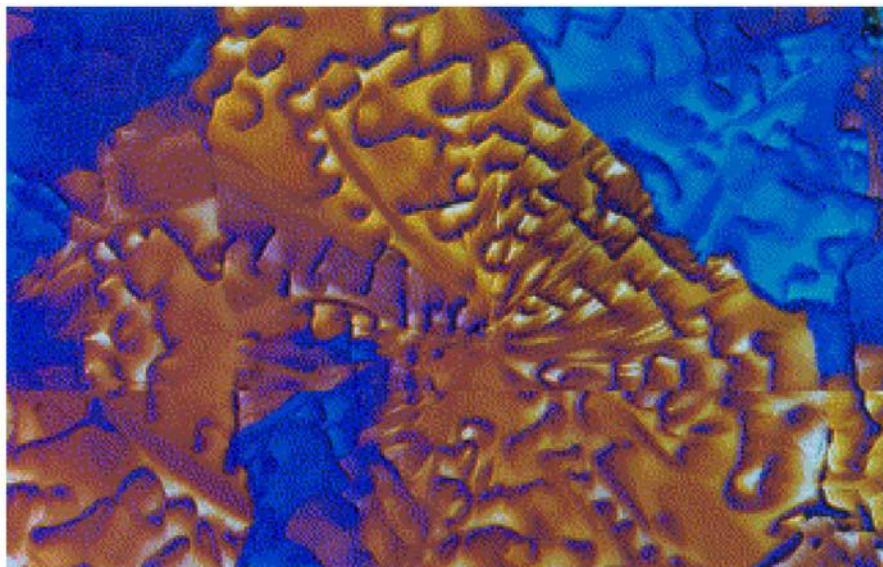


Figure 30. The Schlieren texture of SPO liquid crystal near T_c .

To characterize the liquid crystal behaviors of SPO liquid crystal, we investigated microscopic structural changes by the polarizing microscope and the small-angle XRD spectra during heating and cooling cycle of the film. The SPO liquid crystal showed the Schlieren texture during cooling near T_c (liquid crystalline temperature) as shown in Figure 30.

It also shows the definite distance, 19 Å, between molecules in the wide-angle XRD data in Figure 31. The alignment of molecules in the film near T_c was estimated by an order parameter (S) of the merocyanine dye formed on UV-irradiation of the film. The order parameter of the merocyanine is given by

$$S = (D_{\parallel} - D_{\perp}) / (2 \times D_{\perp} + D_{\parallel})$$

where D_{\parallel} and D_{\perp} are the relative absorption parallel and perpendicular to the molecular orientation, respectively, as shown in Figure 32. The order parameter S was estimated to 0.233, which was similar with the values obtained in previous reports [48-50].

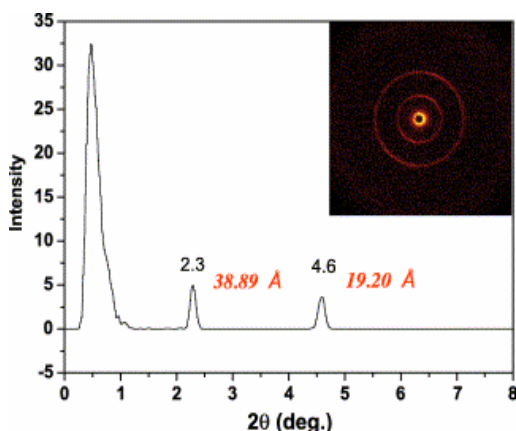


Figure 31. Small-angle spectra of SPO crystal.

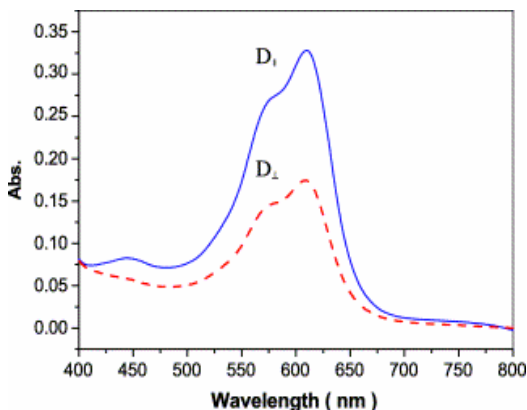


Figure 32. Polarized UV spectra of SPO liquid crystal.

PHOTOSWITCHING OF MULTI-LAYER SELF-ASSEMBLE FILM

Recently, more and more attention has been paid to “layer-by-layer self-assemble” technique in both theoretical and application fields due to its simplicity, versatility, and systematic control of the film structure and thickness. Incorporation of photochromic molecules provides the layer-by-layer self-assembled film with additional interesting properties such as optically induced orientation, linear optical properties, nonlinear optical properties and so on[51-54]. We designed and synthesized a series of spirooxazine dyes and successfully applied them in constructing layer by layer self-assemble ultra thin films switches (Figure 33) [55-57].

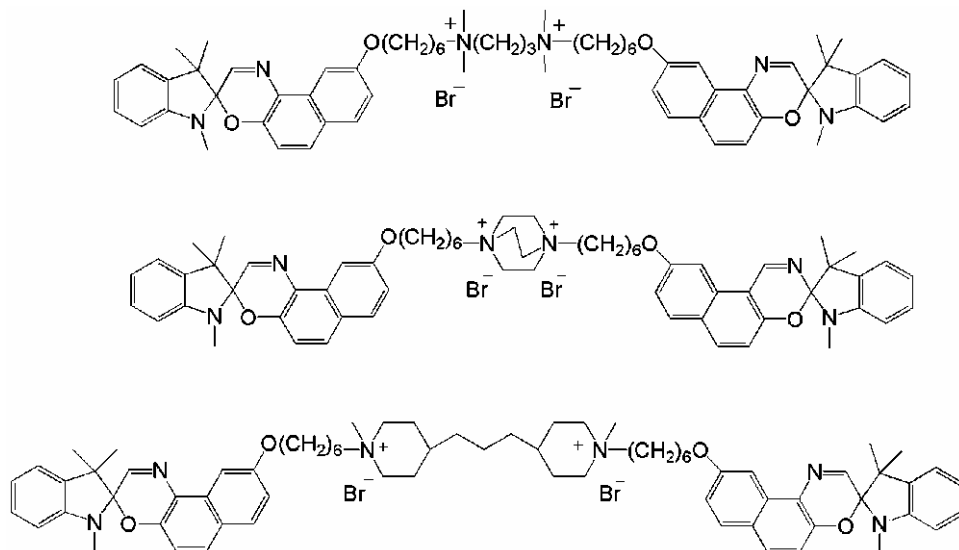


Figure 33. The chemical structure of SPO dyes for layer by layer self-assembly ultra thin films

In generally, one of the most important and universal techniques to construct ultra thin organic films is the alternating assembly of oppositely charged polyelectrolytes, so-called “layer-by-layer self-assemble” method [58-61]. This approach to thin-film deposition involves the assembly of oppositely charged layers of organic materials and can provide a 1-30nm growth step for a bilayer. The layer-by-layer deposition as a simple and versatile method for preparing supported multilayer thin films. The basic process involves dipping a charged substrate into a dilute aqueous solution of an anionic polyelectrolyte and allowing the polymer to absorb and reverse the charge of the substrate surface. The negatively charged substrate is rinsed and dipped into a solution of cationic polyelectrolyte, which absorbs and re-creates a positively charged surface. Sequential absorptions of anionic and cationic polyelectrolytes results in creation of multilayer films. The Figure 34 describes the process of spirooxazine dye layer-by-layer self-assembly deposition. In the first step, a substrate with a negative charged surface is immersed in the solution of the positively charged spirooxazine (SPO). In the second step, the substrate is dipped into the solution containing the negatively charged PSS. By repeating both steps, alternating multilayer are obtained with a precisely repeatable layer thickness.

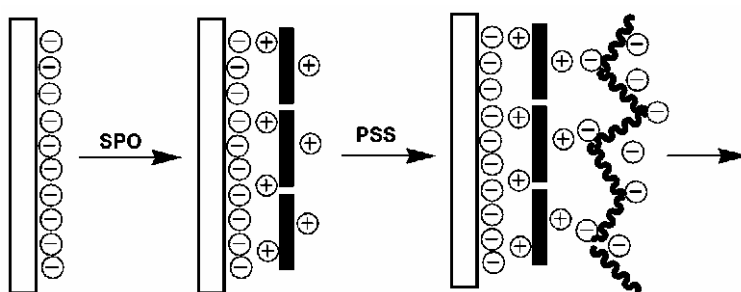


Figure 34. Schematic view of a self alternating multilayer film composed of a cationic spirooxazine and polystyrenesulfonate

A self-assembly multilayer photochromic spirooxazine switch is constructed. Figure 35 showed a self-assembly multilayer photochromic spirooxazine switch on the ITO substrate surface.

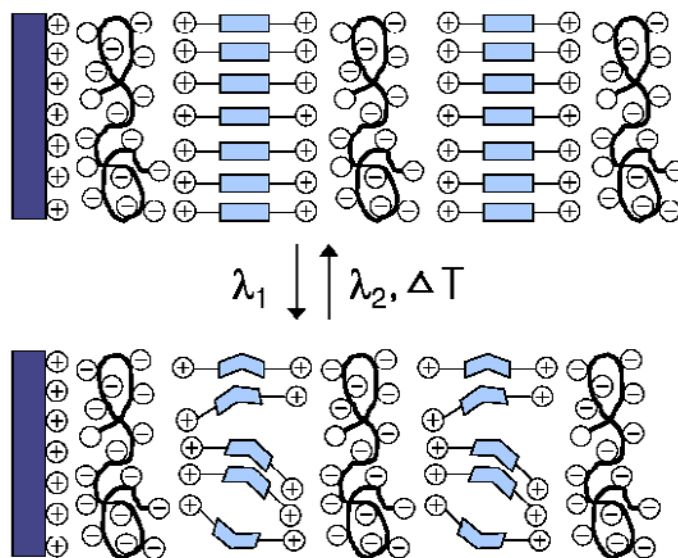


Figure 35. Schematic view of a self alternating multilayer photochromic spirooxazine switch film

The growth of SPO/PSS multilayer films formed by the sequential adsorption of SPO and PSS was examined by using UV-vis spectroscopy. The adsorption spectra upon UV irradiation in self-assembled multilayer containing SPO and PSS are shown in Figure 36. The regularity of the LBL adsorption is demonstrated in the plot of the absorbance of SPO in its maximum at $\lambda_{\max} = 610$ nm versus the number of dipping cycles applied.

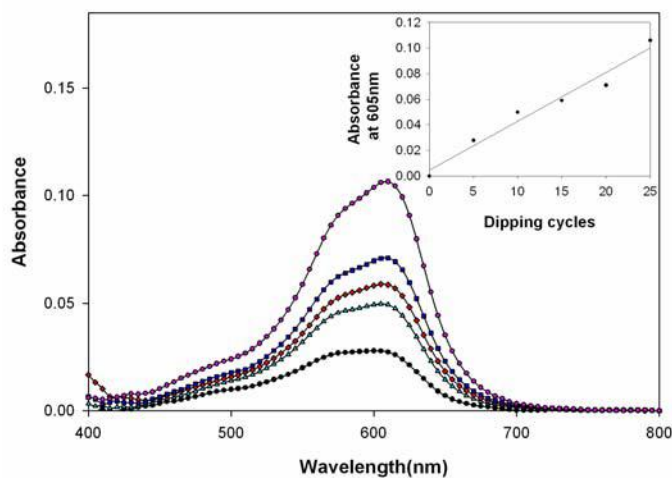


Figure 36. UV-vis absorption spectra of SPO/PSS multilayer films through a consecutive LBL deposition. The insert shows the increase in absorbance at 610 nm as a function of deposition cycles.

More detailed information on the surface structure and the direct image of the self-assembled multilayer on glass surface can also be obtained with AFM. The morphology of 2, 5, 10 pair layer SPO/PSS films was observed by AFM (Figure 37).

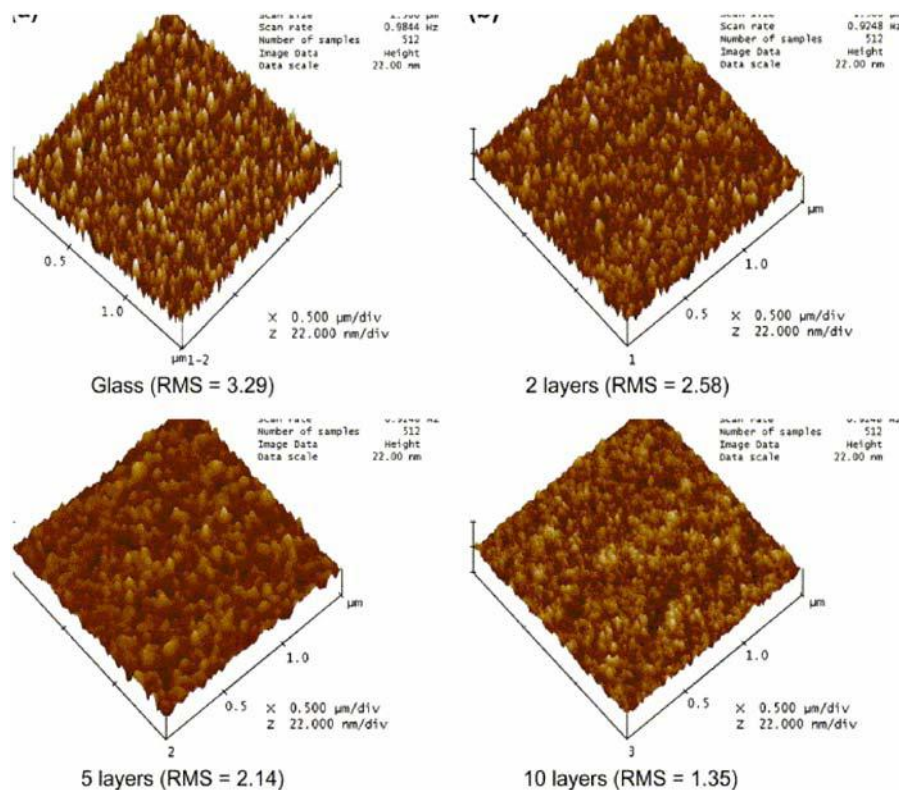


Figure 37. Morphology of the SO/PSS layers: (a) nude glass, (b) 2 layers, (c) 5 layers, and (d) 10 layers.

The mean value of the height from the cross-sectional analysis of raw glass, the surface roughness, RMS, is about 3.29 nm. The roughness of the 2, 5 and 10 pair SPO/PSS multilayer is determined to be 2.58, 2.14 and 1.35 nm, respectively. This decreased surface roughness arises from the stepwise chemical assembly.

PHOTOSWITCHING OF SPIROOXAZINE GEL

Organical gelators have attracted much attention in recent years[62-66]. Hydrogel switch is popular smart materials that can hold large volumes of water, but shrink in volume in the environmental conditions, such as pH, ionic strength, temperature, electric field, and light [67-71]. Such responsive systems are highly desirable in thermo- and mechano-responsive sensor materials or applications like drug delivery or catalysis, or nano- and mesoscopic assemblies with interesting optical and electronic properties and so on[72-74]. We designed and synthesized a bistable photoswitching in poly (N-isopropylacrylamide) with

spironaphthoxazine hydrogel as a new recording media for optical information storage, which have successfully demonstrated erasable and rewritable optical information on the hydrogel [75]. Figure 38 represents the structure and photochemical isomerization of the poly (N-isopropylacrylamide) with spironaphthoxazine hydrogel (abbreviated as PNIPA-SPO-BIS).

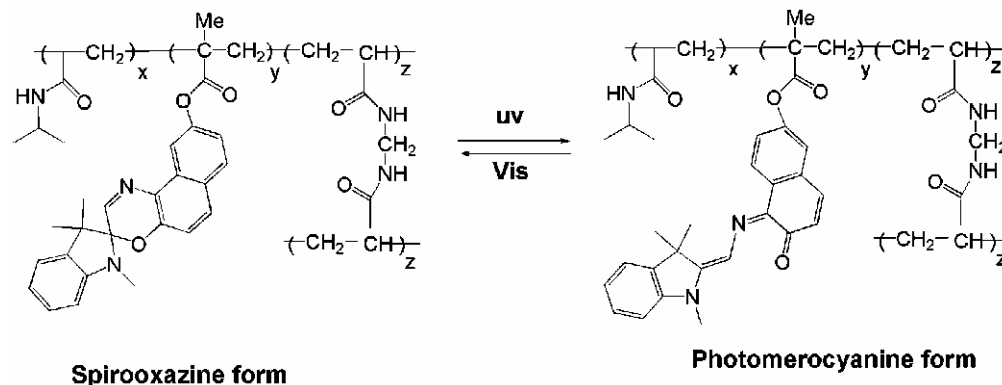


Figure 38. Photoisomerizing behavior of PNIPA-SPO-BIS hydrogel. Left: spirooxazine form; Right: photomerocyanine form

In water, PNIPA-SPO-BIS hydrogel showed excellent photochromic behavior. Figure 39 showed the UV-Vis absorption spectra changes of PNIPA-SPO-BIS copolymer in water solution upon irradiation with UV and Visible light. The inset shows absorption monitoring of cyclical on and off photoconversions of PMMA-SPO-BIS hydrogel in water solution. It can be repeated more than 20 times without any essential loss in color characteristics in repeated on and off process. In addition, we measured the absorption spectral changes of PNIPA-SPO hydrogel to obtain an insight into their photochromic properties in gel phase, which show similarly photochromic performance as in solution (Figure 40). In the same time, the PMMA-SPO-BIS hydrogel showed excellent fatigue resistance.

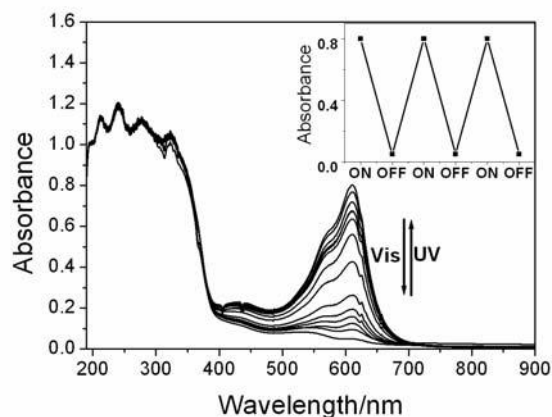


Figure 39. UV-Vis absorption spectra changes of PNIPA-SPO-BIS copolymer in water solution upon irradiation with UV and Visible light. The inset shows absorption monitoring of cyclical on and off photoconversions of copolymer (at $\lambda_{\max}=605\text{nm}$).

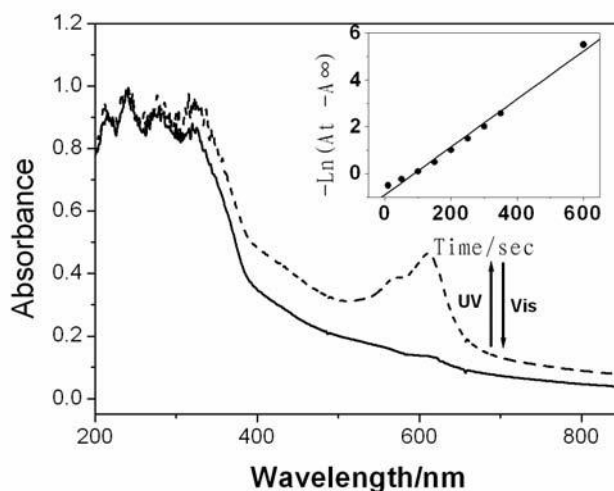


Figure 40. UV-Vis absorption spectra changes of PNIPA-SPO-BIS copolymer in hydrogel state upon irradiation with UV and Visible light at 28°C. The inset shows plot of the decolouration of PNIPA-SPO-BIS hydrogel (at $\lambda_{\text{max}}=615\text{nm}$).

When the PNIPA-SPO-BIS solution is heated above the lower critical solution temperature) value of 30°C (LCST), the transmittance starts to decrease dramatically. The transmittance decreases from 100% at room temperature to 0% at 36°C, and then stabilizes at even higher temperatures. There is no macroscopic phase separation after storage at 40°C for 24 h. when the stabilized PNIPA-SPO-BIS hydrogel is cooled below the LCST value of 31°C from 40°C, the transmittance starts to increase dramatically. When the PNIPA-SPO-BIS hydrogel is cooled at room temperature, it recovers the original PNIPA-SPO-BIS solution. The whole process from **1** state to **2** state is reversible as shown in Figure 41. However, when the PNIPA-SPO-BIS hydrogel was heated from 40 °C to higher temperature, the volume of PNIPA-SPO hdrogel began to shrink and form an agglomerate and separate wholly from the water at 60°C, when the PNIPA-SPO-BIS agglomerate was cooled to at room temperature, which can not recover the original state. This behavior is the typical shrinking change of bulk NIPA copolymer gels in water [76-78]. Interestingly, we use the UV light to irradiate the PNIPA-SPO-BIS agglomerate hdrogel, the red PNIPA-SPO-BIS agglomerate hdrogel turned to blue and kept the color for 2 hour. After visible light irradiation, the blue PNIPA-SPO-BIS agglomerate hdrogel converted back to the initial color. The whole process can repeat more than 15 times and keep the agglomerate from **3** and **4** states (shown in Figure 41).

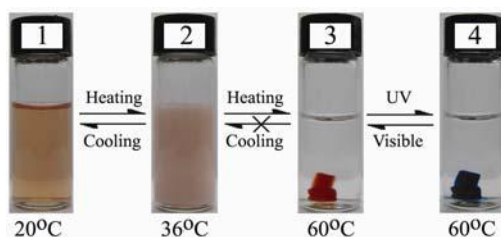


Figure 41. The bistable switching photos of PNIPA-SPO-BIS hydrogel in solution and gel by thermal and light stimuli at different temperature. **1**: Sol (20°C); **2**: Gel (36°C); **3**: Spirooxazine form of Gel (60°C); **4**: Photomerocyanine form of Gel (60°C).

In addition, the morphology of the internal microstructures of the PNIPA-SPO-BIS hydrogels were observed by scanning electron microscopy (SEM). Figure 42 shows the SEM image of the internal microstructure of PNIPA-SPO-BIS hydrogel that the gel has homogeneous porous coral-like microstructure. This morphology indicated that PNIPA-SPO-BIS could form stable hydrogel when the temperature was above the LCST value of PNIPA-SPO-BIS.

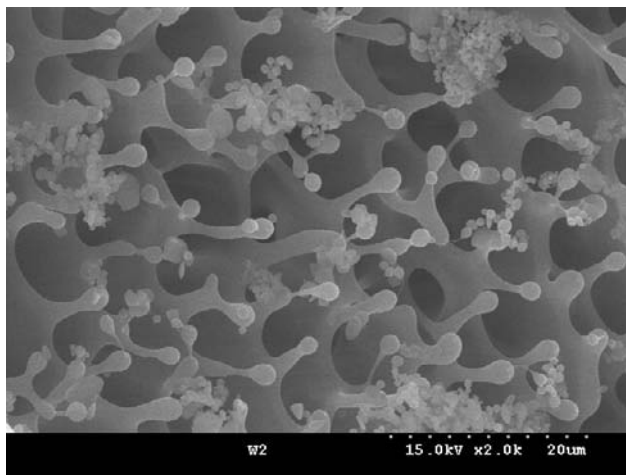


Figure 42. SEM images of PNIPA-SPO-BIS hydrogel. (The gels were prepared from freezing dried in water, PNIPA-SPO-BIS =0.5 wt %).

The inherent characteristics of PNIPA-SPO-BIS hydrogel make it possible to use such materials for data recording. A possible procedure for data recording and erasing is presented in Figure 43 (I). Upon UV light irradiation through the mask, the optical data were recorded on PNIPA-SPO-BIS hydrogel irradiation region. When irradiation with Visible light on irradiation region, the optical data were erased. To obtain visual bistable photoswitching images of PNIPA-SPO-BIS hydrogels, we make the optical storage device that comprised with two slide glasses separated by a 0.1 mm thickness spacer of PET film and placed so as to face each other on the inside of the cell, and the edges of the cell were unsealed. The cell was filled with 0.2% (w/v) PNIPA-SPO-BIS hydrogel water solution. Figure 43 (II) showed the process of the bistable photoswitching in PNIPA-SPO-BIS hydrogel for optical data storage. In gel state, the practical capability of rewritable photoimaging on hydrogel was investigated by patterned illumination through photomasks. The word “KNU”(Kyungpook Nation University abbreviated) was recorded as a first image (Figure 43 C), which was subsequently erased and followed by the recording of a second image, the Korean last name (KIM).The cycles of writing and erasing was repeated more than 20 times. This successful demonstration of rewritable photoimage suggests the potential application of PNIPA-SPO-BIS hydrogel to rewritable optical memory media or imaging processes.

In addition, we have designed and synthesized a multi-switching photochromic poly (N-isopropylacrylamide) with spironaphthoxazine hydrogel copolymer (shown in Figure 44, PNIPA-SPO) [79]. This novel photochromic hydrogel copolymer exhibits excellent reversible photochromic behavior in solution and hydrogel phase undergoes reversible switching process from solution phase to gel phase at a critical temperature (LCST) by thermal

controlling. In addition, this polymer is sensitive to acid and base in water solution, which is promising multiple molecular switches by light, thermal, proton and base stimuli.

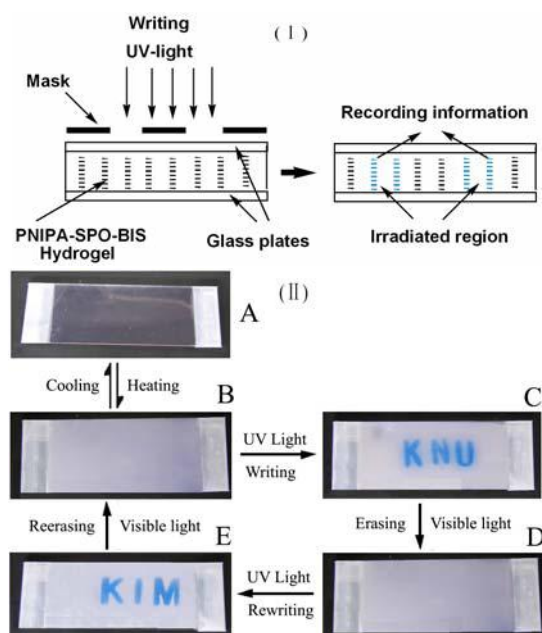


Figure 43. (I) Principle scheme of the optical data recording on PNIPA-SPO-BIS hydrogel. (II) The switching and optical storage images of PNIPA-SPO-BIS hydrogel. A: Sol; B: Gel; C: Writing; D: Erasing; E: Rewriting. Photo-rewritable imaging on the hydrogel by using UV-vis light. The blue regions represent the writing optical data parts irradiated with UV light.

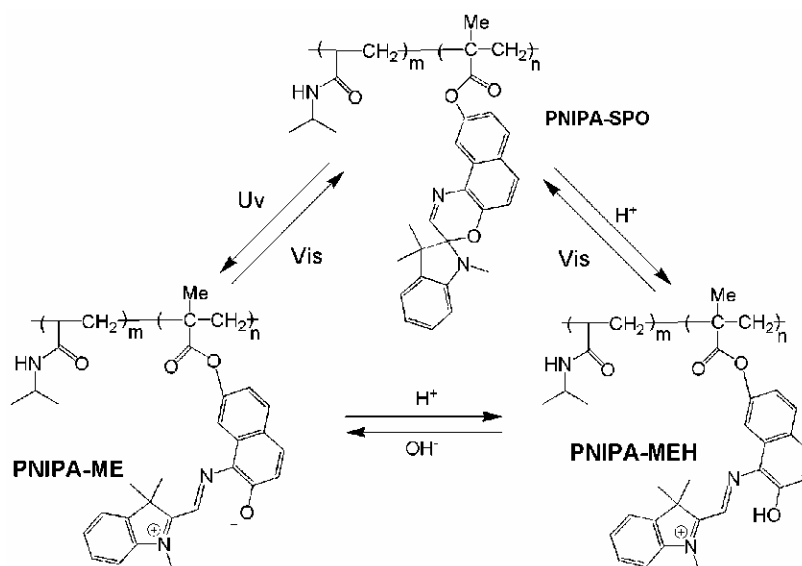


Figure 44. The structure and multiple switching process of photochromic PNIPA-SPO copolymer associated with the three states PNIPA-SPO, PNIPA-ME, and PNIPA-MEH

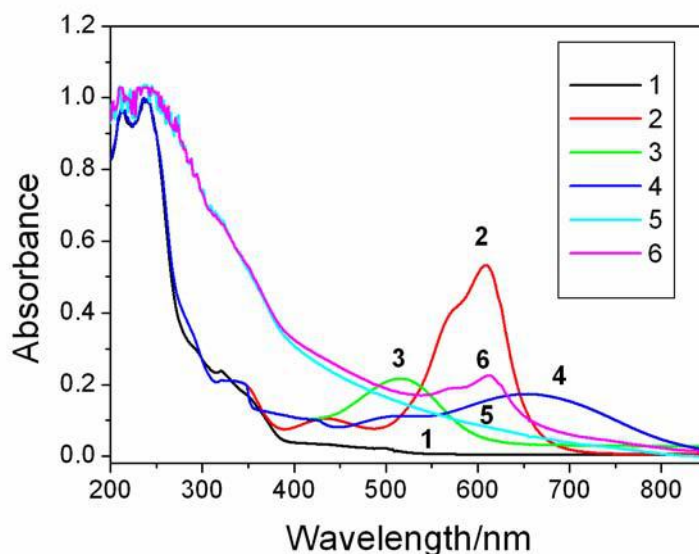


Figure 45. (1) Absorption spectra of multi-switching of PNIPA-SPO copolymer in water solution with the trigger of UV-Vis light, thermal, base, proton.

Figure 45 shows the multi-switching absorption spectral changes of PNIPA-SPO in a water solution and hydrogel by light, proton and base stimuli. Like other spirooxazine molecular, the PNIPA-SPO undergoes reversible photochromic reaction. Irradiation of a water solution of PNIPA-SPO with UV light lead to the appearance of a new absorption band at around 605nm and the colorless solution of PNIPA-SPO turned to blue (shown in Figure 45: line 2). The PNIPA-SPO copolymer showed interesting acidchromic reaction like photochromic compound spiropyran/spirooxazine [80-81]. The interaction of PNIPA-SPO with proton was investigated in water solution through spectrophotometric titration experiment. Upon equivalent proton addition, the colorless solution of PNIPA-SPO became pink red. In Figure 45 line 3 shows the titration spectra of PNIPA-SPO with proton. Upon addition of equivalent H^+ , the band with a peak at round 520nm occurred and produced the protonated merocyanine PNIPA-MEH form. And after visible light irradiation the original absorption spectrum was converted back to the initial state of PNIPA-SPO. Interestingly, upon addition of equivalent OH^- in the solution titrated with proton, the pink solution became blue color. In Figure 45 line 4 showed the absorption spectra of PNIPA-SPO with proton then titration with base. Upon addition of equivalent OH^- , the maximum absorption peak occurred the large red shift and the band with a peak at round 660nm form. And after titrated with proton the original absorption spectrum was converted back to the pink red state of PNIPA-SPO. And after visible light irradiation the original absorption spectrum was converted back to the initial closed-ring isomer of PNIPA-SPO. When a water solution of PNIPA-SPO was heated above the LCST value, the PNIPA-SPO converted from the solution state to hydrogel state. After cooling to at room temperature, the PNIPA-SPO could be recovered the solution state, the whole process was reversible and could be repeated more than 10 times. In addition, we measured the absorption spectra of PNIPA-SPO hydrogel to obtain an insight into their photochromic properties in gel phase, which show resemblely photochromic performance as in solution. The colorless PNIPA-SPO hydrogel turned to blue and a new absorption band

appeared at around 615nm and gradually increased and reached a photostationary state (shown in Figure 45): line 5 gel (closed); line 6 gel (open)). Therefore, the light, thermal proton and base actions may be exploited to modulate the multiple switches between the species PNIPA-SPO, PNIPA-ME and PNIPA-MEH in solution and hydrogel states.

Figure 46 showed the whole multiple switching processes with photographic images of PNIPA-SPO in the trigger of light, thermal, base and proton. Upon irradiation with UV light and visible light, the colorless closed spirooxazine form of PNIPA-SPO can be interconverted with the blue color open-ring PNIPA-ME form in the gel or in solution, i.e. photochromic processes both in hydrogel and in solution. The interconversion between the hydrogel phase and solution could be easily achieved by thermal stimuli at different temperature. In addition, the solution of PNIPA-SPO was both sensitive to proton and base ion, which resulted in obvious changes in the absorption (shown in Figure 45). The reversible chemical switches could be obtained by proton and base stimuli.

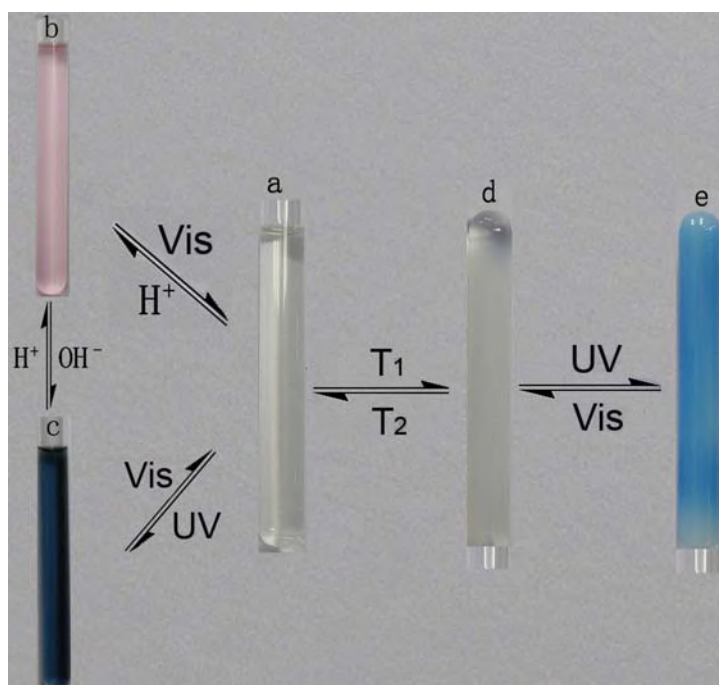


Figure 46. Multiple switching images of PNIPA-SPO copolymer in NMR-tube with the trigger of light, thermal, base, proton. (a) Sol(closed) (b) Sol(closed)+H⁺; (c) Sol(closed)+H⁺+OH⁻; (d) Gel(closed); (e) Gel(open).

CONCLUSION

In this review, we described the recent development of spirooxazine dye as a photoswitching unit in molecular materials, especially spirooxazine single crystal photochromism, spirooxazine dye polymer materials as fluorescence molecular switch, electrical conductivity switch, and viscosity switch. In addition, the layer-by-layer self –

assemble in supermolecular chemistry as a photoswitching unit also is demonstrated. The photochromic spirooxazine dyes show potential applications for ultra-high-density optical information storage, fluorescent molecular probe, and photoregulated molecular switches.

REFERENCES

- [1] B. L. Feringa ed., *Molecular Switches*, Wiley-VCH, Weinheim, 2001.
- [2] V. Balzani, A. Credi, M. Venturi, *Molecular Devices and Machines: A Journey into the Nano World*, Wiley-VCH, Weinheim, 2003.
- [3] H. Dürr, H. Bouas-Laurent In: *Photochromism: Molecules and Systems*, Eds., Elsevier: Amsterdam, 1990.
- [4] J. C. Crano, R. J. Gugliemetti, *Organic Photochromic and Thermochromic Compounds*, New York: Plenum, 1999.
- [5] V. I. Minkin, *Chem. Rev.*, 2004, 104(5), 2751-2776.
- [6] G. Berkovic, V. Krongauz, V. Weiss, *Chem. Rev.*, 2000, 100(5), 1741-1754.
- [7] V. Lokshin, A. Samat, A.V. Metelitsa, *Russ. Chem. Rev.* 2002, 71, 893.
- [8] F. M. Raymo, *Chem. Soc. Rev.* 2005, 34, 327.
- [9] F. M. Raymo and Massimiliano Tomasulo, *Chem. Eur. J.*, 2006, 12, 3186-3193
- [10] H. Tian, S. J. Yang, *Chem. Soc. Rev.*, 2004, 33, 85-.
- [11] H. Tian and S. Wang, *Chem. Commun.*, 2007, 8: 781-792.
- [12] M. Irie, *Photo-Reactive Materials for Ultrahigh-Density Optical Memories*; Elsevier: Amsterdam, 1994.
- [13] A. Toriumi, S. Kawata, M. Gu, *Opt. Lett.*, 1998, 23, 1924-1926.
- [14] S. Kobatake, S. Takami, H. Muto, T. Ishikawa, M. Irie, *Nature*, 2007, 446, 778-781.
- [15] S. L. Gilat, S. H. Kawai, J.-M. Lehn, *Chem. Eur. J.*, 1995, 1, 275-284.
- [16] K. Matsuda, M. Irie, *J. Am. Chem. Soc.*, 2001, 123, 9896-9897.
- [17] S. Kobatake, T. Yamada, K. Uchida, N. Kato, M. Irie, *J. Am. Chem. Soc.*, 1999, 121, 2380-2386.
- [18] S. Kobatake, M. Yamada, T. Yamada, M. Irie, *J. Am. Chem. Soc.*, 1999, 121, 8450-8456.
- [19] M. Morimoto, S. Kobatake, M. Irie, *Chem. Eur. J.*, 2003, 9, 621-627.
- [20] M. Irie, S. Kobatake, M. Horichi, *Science*, 2001, 291, 1769-1772.
- [21] G. P. Dinesh, B.B. Jason, A. K. Roni and L. F. Natia, *Chem. Commun.*, 2005, 2208-2210.
- [22] K. Chamontin, V. Lokshin, A. Samat, R. Gugliemetti, R. Dubest and J. Aubard, *Dyes Pigments*, 1999, 43, 119.
- [23] W. Clegg, N. C. Norman, T. Flood, L. Sallans, W. S. Kwak, P. L. Kwiatkowski and J. G. Lasch, *Acta Crystallogr., Sect. C*, 1991, 47, 817.
- [24] R. Millini, G. del Piero, P. Allegrini, L. Crisci and V. Malatesta, *Acta Crystallogr., Sect. C*, 1991, 47, 2567.
- [25] J.-P. Reboul, A. Samat, P. Lareginie, V. Lokshin and R. Gugliemetti, *Acta Crystallogr., Sect. C*, 1995, 51, 1614.
- [26] H.-J. Suh, W.-T. Lim, J.-Z. Cui, H.-S. Lee, G.-H. Kim, N.-H. Heo and S.-H. Kim *Dyes Pigments*, 2003, 57(2), 149-159

- [27] G. R. Desiraju., T. Steiner, *The weak hydrogen bond*. Oxford University
- [28] M. Irie, T. Fukaminato, T. Sasaki, N. Tamai, T. Kawai, *Nature*, 2002, 420, 759–760.
- [29] L. Zhu, W. Wu, M.-Q. Zhu, J. J. Han, J. K. Hurst, A. D. Q. Li, *J. Am. Chem. Soc.*, 2007, 129(12), 3524-3526.
- [30] X. L. Meng, W. H. Zhu, Z. Q. Guo, J. Q. Wang, and H. Tian, *Tetrahedron*, 2006, 62, 9840.
- [31] W. Yuan, L. Sun, H. Tang, Y. Wen, G. Jiang, W. Huang, L. Jiang, Y. Song, H. Tian, D. Zhu, *Adv. Mater.*, 2005, 17, 156.
- [32] S. Wang, C.Y. Yu, M. S. Choi and S.-H. Kim, *Dyes Pigments*, 2008, 77(1), 245-248.
- [33] S. Wang, C.Y. Yu, M. S. Choi and S.-H. Kim, *J. Photochem. Photobio. A: Chem.*, 2007, 192(1), 17-22.
- [34] A. J. Myles, B. Gorodetsky, N. R. Branda, *Adv. Mater.* 2004, 16, 922.
- [35] Philp and J. F. Stoddart, *Angew. Chem., Int. Ed. Engl.*, 1996, 35, 1154.
- [36] J. W. Steed and J. L. Atwood, *Supramolecular Chemistry*, Wiley, Chichester, 2000.
- [37] M. S. Vollmer, T. D. Clark, C. Steinem and M. R. Ghadiri, *Angew. Chem., Int. Ed.*, 1999, 38, 1598.
- [38] M. Irie, A. Menju, K. Hayashi, *Macromolecules*, 1979, 14, 262.
- [39] S.-H. Kim, S.-Y. Park, N.-S. Yoon., S.-R. Keum, K. Kohc, *Dyes Pigments*, 2005, 66,155-160.
- [40] B. Delley, *J. Chem. Phys.*, 1990, 92, 508-517.
- [41] B. Delley, *J. Chem. Phys.*, 2000, 113, 7756-7764.
- [42] S.-H. Kim, S.-Y. Park, C.-J. Shin and N.-S. Yoon, *Dyes Pigments*, 2007, 72(3), 299-302.
- [43] J. P. Perdew, K. Burke, M. Ernzerhof, *Phys. Rev. Lett.*, 1996, 77, 3865.
- [44] A. D. Boese, N.C. Handy, *J. Chem. Phys.*, 2001, 114, 5497-5503.
- [45] C. Denekamp, B. L. Feringa, *Adv. Mater.*, 1998, 10(14), 1080-1082.
- [46] S. H. Chen, H. M. P. Chen, Y. Geng, S. D. Jacobs, K. L. Marshall, T. N. Blanton, *Adv. Mater.*, 2003, 15(13), 1061-1065.
- [47] J.-H. Park, S.-H. Kim and J.-H. Kim, *Mater. Sci. Engineer. C*, 2004, 24(1-2), 275-279.
- [48] F. P. Shvartsman, V. A. Krongauz, *J. Phys. Chem.* 1984, 88, 6448.
- [49] L. Shragina, F. Buchholtz, S. Yizchaik, V. Krongauz, *Liq. Cryst.* 1990, 7, 643.
- [50] F. P. Shvartsman, V. A. Krongauz, *Nature*, 1984, 309, 608.
- [51] G. Decher, *Science*, 1997, 277, 1232.
- [52] P. Bertrand, A. Jonas, A. Laschewsky. *Macromol. Rapid. Commun.*, 2000, 21, 319.
- [53] P. T. Hammond, *Curr. Opin. Colloid. Interface. Sci.*, 2000, 4, 430.
- [54] X. Zhang, J. C. Shen, *Adv. Mater.*, 1999, 11,1139.
- [55] S.-H. Kim, C.-J. Shin, M.-S. Choi and S. Wang, *Dyes Pigments*, 2008, 77(1) , 70-74.
- [56] S.-H. Kim, C.-J. Shin, S.-R. Keum and K. Koh, *Dyes Pigments*, 2007, 72(3), 378-382.
- [57] S.-H. Kim, C. Yu, C.-J. Shin and M.-S. Choi, *Dyes. Pigments*, 2007, 75(1), 250-252.
- [58] A. Ulman, *From Langmiur-Blodgette to self-assembly*. Boston/New York/Tronto: Academic Press., 1991, p.440.
- [59] G. Decher, J. D. Hong. *Makromol. Chem. Macromol. Symp.*, 1991, 46, 321.
- [60] Y.-A. Son, Y.-M. Park, C.-J. Shin and S.-H. Kim, *Dyes Pigments*, 2007, 72(3), 345-348.
- [61] S.-H. Kim, C.-H. Ahn, S.-Y. Park, C.-J. Shin and H.-J. Suh, *Dyes Pigments*, 2006, 69(1-2), 108-110.

- [62] J. H. van Esch, B. L. Feringa, *Angew. Chem. Int. Ed.*, 2000, 39, 2263.
- [63] D. J. Abdullah, R. G. Weiss, *Adv. Mater.* 2000, 12, 1237;
- [64] Maaïke de Loos, B. L. Feringa, J. H. van Esch, *Eur. J. Org. Chem.* 2005, 3615.
- [65] M. S. Neralagatta, M. Uday, *Chem. Soc. Rev.*, 2005, 34, 821.
- [66] K. Sugiyasu, N. Fujita, S. Shinkai, *Angew. Chem., Int. Ed.* 2004, 43, 1229.
- [67] M. Lei, Y. Gu, A. Baldi, R. A. Siegel, B. Ziaie, *Langmuir*, 2004, 20, 8947.
- [68] G. M. Eichenbaum, P. F. Kiser, S. A. Simon, D. Needham, *Macromolecules*, 1998, 31, 5084.
- [69] M. E. Harmon, M. Tang, C. W. Frank, *Polymer*, 2003, 44, 4547.
- [70] T. Tanaka, I. Nishiq, S. Sun, S. Ueno-Nishio, *Science*, 1982, 218, 467.
- [71] A. Suzuki, T. Tanaka, *Nature*, 1990, 346.
- [72] J. B. Beck, S. J. Rowan, *J. Am. Chem. Soc.*, 2003, 125, 13922.
- [73] N. Fujita, M. Asai, T. Yamashita, S. Shinkai, *J. Mater. Chem.* 2004, 14, 2106.
- [74] M. Numata, K. Sugiyasu, T. Hasegawa, S. Shinkai, *Angew. Chem., Int. Ed.*, 2004, 43, 3279.
- [75] S. Wang, M.-S. Choi and S.-H. Kim, *J. Photochem. Photobio. A: Chemistry*, 2008, in press.
- [76] X. J. Chen, and K. Tsujii, *Macromolecules*, 2006, 39, 8550.
- [77] H. Yan, H. Fujiwara, K. Sasaki, and K. Tsujii, *Angew. Chem. Int. Ed.*, 2005, 44, 1951.
- [78] A. Kacmaz, G. Gurdag, *Macromol. Symp.*, 2006, 239, 138.
- [79] S. Wang, M.-S. Choi and S.-H. Kim, *Dyes Pigments*, 2008, 78(1), 8-14.
- [80] F. M. Raymo, S. Giordani, *J. Am. Chem. Soc.*, 2001, 123(19), 4651-4652
- [81] E. B. Gaeva, V. Pimienta, S. Delbaere, A. V. Metelitsa, N. A. Voloshin, V. I. Minkin, G. Vermeersch and J. C. Micheau, *J. Photochem. Photobio. A: Chemistry*, 2007, 191(2-3), 114-121.